

WIND-TUNNEL STUDY OF  
WIND LOADS ON PHOTOVOLTAIC STRUCTURES--  
PHASE II

by

M. Poreh,\* J. A. Peterka\*\*  
and J. E. Cermak\*\*\*

for

Bechtel National, Inc.  
P.O. Box 3963  
San Francisco, California 94119

Fluid Mechanics and Wind Engineering Program **Engineering Sciences**  
Fluid Dynamics and Diffusion Laboratory  
Department of Civil Engineering  
Colorado State University  
Fort Collins, Colorado 80523

APR .1 1982

CSU Project 5-36060

January 1982

U18401 0076207

\*Visiting Professor (from Department of Civil Engineering,  
Technion, Haifa, Israel)  
\*\*Associate Professor  
\*\*\*Professor-in-Charge, Fluid Mechanics and  
Wind Engineering Program

CER81-82MP-JAP-JEC21

## ACKNOWLEDGEMENTS

The authors would like to acknowledge the contributions of Mr. Morgan Downing to the experimental and data acquisition work. The help of Mr. Noriaki Hosoya should also be acknowledged.

Further, the authors would like to thank Dr. Andy Franklin and Mr. Nathan Kotlyar from Bechtel National for their cooperation in establishing the project and in aiding development of a test plan.

## TABLE OF CONTENTS

<u>Chapter</u>		<u>Page</u>
	ACKNOWLEDGEMENTS . . . . .	i
	LIST OF FIGURES . . . . .	iii
	LIST OF SYMBOLS . . . . .	v
1	INTRODUCTION . . . . .	1
2	EXPERIMENTAL CONFIGURATION, INSTRUMENTATION AND DATA ACQUISITION . . . . .	2
3	ANALYSIS OF THE EXPERIMENTAL RESULTS . . . . .	6
	3.1 The Single Array Tests . . . . .	6
	3.2 The Array Field Tests . . . . .	6
	3.2.1 The Normal Force Coefficient . . . . .	7
	3.2.2 The Pitching Moment Coefficients . . . . .	9
	3.2.3 The Yawing Moment Coefficients . . . . .	9
4	CONCLUSIONS . . . . .	10
	REFERENCES . . . . .	11
	FIGURES . . . . .	12
	APPENDIX A--AERODYNAMIC COEFFICIENTS FOR PHOTOVOLTAIC ARRAYS . . . . .	35

## LIST OF FIGURES

<u>Figure</u>		<u>Page</u>
1	A view of the array field model and fence in the Meteorological Wind Tunnel (configuration NFA4) . . .	13
2	Roughness configuration in the Meteorological Wind Tunnel for generating a 1/7 power law (NEWBYL) near the metric array . . . . .	14
3	Velocity distribution in the test section . . . . .	15
4	Mean velocities and turbulent intensities in the lower section of the boundary layer . . . . .	16
5	A view of the 6-component balance system and the 1:24 scale model . . . . .	17
6	Conceptual low-cost support for a photovoltaic array . . . . .	18
7	Directions of forces and moments for northerly and southerly winds . . . . .	19
8	The values of CN and CMZ in the present and the previous study (1979), H = 2.0 ft . . . . .	21
9	The values of CN and CMZ for H = 2.0 ft and H = 1.5 ft . . . . .	22
10	The values of CMS for H = 2.0 ft and H = 1.5 ft . . . . .	23
11	Distribution of $ CN  \times 100$ in the field (left number, without fence; right number, with fence) . . . . .	24
12	Comparison of values of $ CN  \times 100$ for H = 1.5 ft (left) and H = 2.0 ft (right) without a fence . . . . .	26
13	Comparison of values of $ CN  \times 100$ for fenced fields with H = 1.5 ft (left) and H = 2.0 ft (right) . . . . .	27
14	Maximum values of $ CN  \times 100$ without a fence for all wind directions for H = 1.5 ft (left) and H = 2.0 ft (right) . . . . .	29

<u>Figure</u>		<u>Page</u>
15	Maximum values of $ CN  \times 100$ with a fence (and a corner fence) for all wind directions for $H = 1.5$ ft (left) and $H = 2.0$ ft (right) . . .	29
16	Distribution of $ CMZ  \times 100$ in the field (left number--without fence, right number-- with fence) . . . . .	30
17	Distribution of $ CMS  \times 100$ in the field (left number--without fence, right number-- with fence) . . . . .	32
18	Notation used for array location and field test files . . . . .	34

## LIST OF SYMBOLS

<u>Symbol</u>	<u>Definition</u>
A	Array surface area = 192 sq ft in prototype
C	Array chord length = 8 ft in prototype
CFX	Force coefficient in X-direction
CFY	Force coefficient in Y-direction
CMS	Moment coefficient about S-axis
CMX	Moment coefficient about X-axis
CMY	Moment coefficient about Y-axis
CMZ	Moment coefficient about Z-axis
CN	Normal force coefficient
DXY	= C/2
ES	Normalized eccentricity by DXY for MZ
EZ	Normalized eccentricity by DXY for MS
FN	Normal force
FX	Force in X-direction
FY	Force in Y-direction
H	Ground clearance
HF	Fence height
MS	Moment about S-axis (yawing moment)
MX	Moment about X-axis
MY	Moment about Y-axis
MZ	Moment about Z-axis (pitching moment)
$Q_{REF}$	Reference dynamic pressure
S	Center chord of the photovoltaic array
$U_{REF}$	Reference wind velocity
WD	Wind direction
$\beta$	Tilt angle
$\rho$	Density of air

## 1. INTRODUCTION

The present work is a continuation of a previous study on the magnitude of wind loadings on photovoltaic arrays.<sup>(1)</sup> A series of wind-tunnel tests were conducted in that study to determine the effect of various design parameters on the wind loadings for different wind directions and wind profiles on a single array and on individual arrays at different locations in a large array field. The tests showed that arrays at the upwind edges and corners of the field are subjected to very large loadings, but that these loadings can be drastically reduced by fences designed to act as wind barriers. No measurements of the relative effect of the fence further in the field were made. All the previous array field tests were conducted with a "standard array configuration" (see Figure 6) in which the height of the arrays above ground was  $H = 2.0$  ft.

Subsequent analysis of the wind-tunnel data by Bechtel National, Incorporated, showed that it might be advantageous to use a smaller array height,  $H = 1.5$  ft, and that in many situations the use of fences for reducing the wind loadings on the upwind edges and corners of the field would not be economical.

It was therefore decided to extend the previous study and to examine more closely the mean forces and moments on individual arrays in the field with  $H = 1.5$  ft, with and without a fence. The tests were performed in a  $1/7$  power-law boundary layer (BL1) at which the highest loads had been observed. The fence used in the study had 30 percent porosity and an additional corner fence (see [1], Figure 26).

The results of the present investigation are presented in a ready-to-use form, adopting the previously defined aerodynamic dimensionless force and moment coefficients and notation.

## 2. EXPERIMENTAL CONFIGURATION, INSTRUMENTATION AND DATA ACQUISITION

The tests were conducted in the Meteorological Wind Tunnel of the Fluid Dynamics and Diffusion Laboratory at Colorado State University in which the earlier study was performed, using the 1:24 scale array (Figure 1). Some changes have been made in the wind tunnel since 1979 and a different upstream roughness configuration (see Figures 1 and 2) had to be installed in the tunnel to obtain a  $1/7$  power law at the test section. One of the changes was the installment of a larger turntable which made it possible to rotate most of the array field model as one unit. This has, however, resulted in a slight dependence of the equivalent roughness in the neighborhood of the model on the wind direction which could cause a 2 to 3 percent change of the mean local velocities very close to the floor (1 to 2 in.) which might affect the single array tests. Figure 3 compares the velocity profiles at the test section (NEWBYL) with the profile measured in 1979 (OLDBYL). The dimensionless velocity profiles were normalized by the velocity at 50 in. above the floor. Figure 4 shows the velocity distributions in the lower portion of the boundary layer. The velocity at  $H = 10$  in. was used to normalize the profiles in this graph. The old and the new velocity distributions appear to be very similar but small differences between them exist. Although these differences can affect the values of the aerodynamic coefficients by a few percent, they are undoubtedly small compared to the observed differences in the atmospheric velocity distributions above apparently similar smooth sites.

The mean force and moment measurements on the instrumented model were made with a new 6-component balance designed by G. K. Keily and J. A. Peterka.<sup>(2)</sup> Figure 5 shows a view of the new balance and the



metric array connected to it. The vanes which are attached to the bottom of the balance were submerged in a viscous oil bath to damp vibrations of the array. The balance was designed to measure relatively small forces and moments of the order of 1 lb- and 3 lb-in. Its load-voltage coefficients and its axes of zero moments were determined by a careful calibration prior to the tests. Frequent checks of its response were also made during the course of the tests. Since the balance used in the previous study was a 50-lb balance which worked at the lower part of its useful range, it is estimated that this could have caused relatively larger scatter and errors in the moment measurements and that the present moment measurements are much more reliable.

The use of the new balance made it possible to measure, in addition to the normal force and pitching moment coefficients CN and CMZ, the yawing moment coefficient on the structure CMS around the center chords of the array S (see Figures 6 and 7). The pitching and yawing moments were then used to calculate the displacement of the normal force from the center of the balance, which will be designated by ES and EZ (see Figure 7). Note that the sign of ES and EZ is determined by the sign of both the moments and the normal forces. The same mean dynamic pressure  $Q_{REF}$  ( $= 1/2\rho U_{REF}^2$ ) at the reference height of 30 ft was used in this study so that the dimensionless coefficients given in the report are:

$$CN = \frac{FN}{Q_{REF} \cdot A} \quad (1)$$

$$CMZ = \frac{MZ}{Q_{REF} \cdot A \cdot DXY} \quad (2)$$

$$ES = - \frac{CMZ}{CN} \quad (3)$$

$$CMS = \frac{MS}{Q_{REF} \cdot A \cdot DXY} \quad (4)$$

$$EZ = \frac{CMS}{CN} \quad (5)$$

where A is the area of the array (192 sq ft in the prototype) and  $DXY = C/2$  is half the chord length of the array ( $C = 8$  ft in the prototype). The normal force was calculated using the equation

$$FN = FX \cdot \sin 35^\circ - FY \cdot \cos 35^\circ \quad (6)$$

where FX and FY are the forces in X- and Y-direction as shown in Figure 7 respectively.

It should be stressed that the shape of the array which resembles to a large extent that of a flat plate ensures the resultant force on the array is practically equal to the normal force FN. Thus the coefficients of FX and FY on the array can be determined by

$$|CFX| = |CN| \sin \beta \quad (7)$$

$$|CFY| = |CN| \cos \beta \quad (8)$$

where  $\beta$  in the present study is  $35^\circ$ .

The moment coefficients acting on the arrays CMX, CMY and CMZ (see Figure 7) are determined by the position of the resultant force FN and are given by

$$CMZ = CN \cdot ES \quad (9)$$

and

$$CMS = CN \cdot EZ = \frac{CMY}{\sin 35^\circ} = \frac{CMX}{\cos 35^\circ} \quad (10)$$

where MS is the moment around the S axis (see Figure 7).

In the above equations we have used the values of  $|CFX|$  and  $|CFY|$  since the sign of FX and FY varies with the wind direction. Note

that  $F_X$  is defined as the force in either the south or the north direction and not in the direction of the wind.

The above calculations are, however, correct only within an error of approximately 5 percent in the force coefficient calculations and 10 percent in the moment calculations.

### 3. ANALYSIS OF THE EXPERIMENTAL RESULTS

#### 3.1 The Single Array Tests

The single array tests were made for comparing the data obtained in the present and the previous report to examine the effect of the reduced array height  $H$  from  $H = 2.0$  ft to  $H = 1.5$  ft and to measure the yawing moment coefficient  $C_{MS}$ , which was not measured in the previous study. The data for the single array runs is tabulated at the end of the report in Files S20 and S15. Figure 8 compares the previous and the new measurements for  $H = 2.0$  ft. The agreement between the  $C_N$  data is satisfactory in view of the slight changes in the velocity profile. The data confirms the previous observation that the maximum value of  $C_N$  is obtained around a wind direction of  $45^\circ$ .

Larger differences exist, however, between the present and the earlier measurements of the pitching moment coefficient  $C_{MZ}$ . As explained earlier the previous measurements are less reliable than the present ones.

Figures 9 and 10 compare the aerodynamic coefficients of the single array for  $H = 2.0$  ft and  $H = 1.5$  ft. The dependence of the coefficients on the wind direction is very similar. A small reduction in the values of the coefficients is observed for  $H = 1.5$  ft. As one sees from the yawing moment coefficient the maximum moment around the  $S$  axis occurs around wind directions of  $45^\circ$  and  $135^\circ$ . Slightly larger moments are observed for the southerly winds.

#### 3.2 The Array Field Tests

The results of the array field tests are tabulated in the Appendix at the end of the report using the notation shown in Figure 18. The data is also presented in Figures 11 through 17 using a schematic

description of the array field. The  $H = 2.0$  ft data are from the Phase I study.

### 3.2.1 The Normal Force Coefficient

The measurements of the normal force coefficients showed that all the coefficients measured at the northeast corner of the field for wind directions  $0^\circ$ ,  $30^\circ$ ,  $45^\circ$  and  $60^\circ$  are negative, indicating an upward lift. Similarly, all the coefficients measured at the southwest corner of the field are positive, except for a few cases in which the absolute value of  $CN$  is very small. We shall therefore refer in the following discussion to the absolute value of the normal force coefficient expressed in percent  $|CN| \times 100$ .

Figure 11 shows the values of  $|CN| \times 100$  measured in 176 runs. Each section of these figures shows the values measured at the northeast corner for one wind direction together with the values measured at the southwest corner for the opposite wind direction;  $WD = 0^\circ$  and  $180^\circ$ ,  $30^\circ$  and  $210^\circ$ , etc. Two numbers are shown in the space allocated for each array. The left-hand number shows the value of  $|CN| \times 100$  for the field without a fence and the right-hand number shows the value of  $|CN| \times 100$  for the fenced field. The 30 percent porosity fence used in this study was always augmented at the corners by the corner fence used in the previous study (see [1], Figure 26). Figure 26 also shows the spacings between the rows and the distances to the fence. The height of the fence in the prototype was  $HF = 5$  ft.

One sees from Figure 11 that the normal force coefficients recorded at the upwind edges of the unfenced field were close to those recorded in the single array tests and that the largest value  $CN = -0.79$ , was

recorded at the corner of the northeast field. Slightly smaller values were recorded at the east and west edges of the field.

A drastic reduction in the absolute values of the normal force coefficients is observed in the inner part of the field where a maximum of  $CN = -0.27$  was recorded at array B2 for  $WD = 30^\circ$ . Significantly lower values are observed for southerly winds.

Figure 12 compares the values of  $|CN|$  obtained in the unfenced field in the present study for  $H = 1.5$  ft with those obtained in the unfenced field previously with  $H = 2.0$  ft. In general the  $H = 2.0$  ft values are larger. The only significant difference is at array NC2. (The arrays denoted by 1,2,3,4,5,6,7 and 8 in the previous report are being denoted now by A1,C1,A2,C2,A4,C4,A7 and C7.)

The use of a 5-ft high fence, with a corner fence, has drastically reduced the values of the normal force coefficients on the array facing the wind. The fence was particularly helpful when the wind was normal to it. It was not very effective, however, in reducing side winds. The normal force coefficients on the east side were, in some cases, even higher than in the unfenced field probably due to the effect of the corner fence. The fence has also increased the values of some of the coefficients inside the field.

Figure 13 compares the normal coefficients measured in the present study with those measured in the previous study ( $H = 2.0$  ft). Some of the values from the previous study were measured without a corner fence. These are denoted by an asterisk.

The order of magnitude and the distribution of the two sets of data appear to be quite similar. One sees, for example, that the increase in the values of the coefficients from array C2 to array C4 and array C7

for wind direction  $45^\circ$  exists in both cases and that the relatively high value of  $|CN|$  at C7 was not due to an experimental error.

Figures 14 and 15 show the maximum value of  $|CN|$  obtained at each array for all wind directions for the unfenced field and for the fenced field.

### 3.2.2 The Pitching Moment Coefficients

The pitching moment coefficients in the unfenced field were generally low, see Figure 16. The maximum value recorded was  $|CMZ| = 0.09$  at the southern edge of the field for wind directions  $180^\circ$  and  $210^\circ$ . The values of  $CMZ$  in the fenced field were practically zero.

### 3.2.3 The Yawing Moment Coefficients

The distributions of the yawing moment coefficient are shown in Figure 17. Very small values of  $|CMS|$  were recorded for  $WD = 0^\circ$  and  $180^\circ$ . Larger values were recorded at the west edge of the field for  $WD = 210^\circ$  and very large moments were recorded at the same edge for  $WD = 225^\circ$ . The reason for these large moments is that only one side of these arrays is exposed to the wind. A similar effect is noticed in the eastern edge for  $WD = 45^\circ$ , but apparently the protection provided by upwind arrays in this case is larger.

The fence appears to reduce to one-half the large moments recorded on the west side for  $WD = 225^\circ$ , as well as the rest of the large moments in the field. However, in some cases small amplifications of  $|CMS|$  are observed, as in arrays SFB2 and SFB3.

#### 4. CONCLUSIONS

The measurements made in the present study appear to be consistent with those made in the previous study and a clear picture of the loadings in the field emerges.

In the unfenced field one can divide the field into two parts; the edges of the field where the values of  $|CN|$  are larger than 0.30 and reach a maximum near 0.8, and the inner part of the field where  $|CN| < 0.30$ . The yawing moment is also large only in the arrays at the edges of the field.

The introduction of a fence with a corner fence reduces the high loadings on the outer arrays to a maximum of  $|CN| = 0.37$  and also reduces the very large yawing moments in the field. However, the fence slightly increases the loadings on some inner arrays. Thus, the loadings on the entire fenced field appear to be approximately of the same order of magnitude for design purposes.



## REFERENCES

1. Poreh, M., J. A. Peterka, and J. E. Cermak, Wind-tunnel study of wind loads on photovoltaic structures, Colorado State University Report No. CER79-80MP-JAP-JEC12, September 1979, 89 p.
2. Keily, G. K., Unpublished report describing a project prepared under the supervision of Professor J. A. Peterka.

**FIGURES**

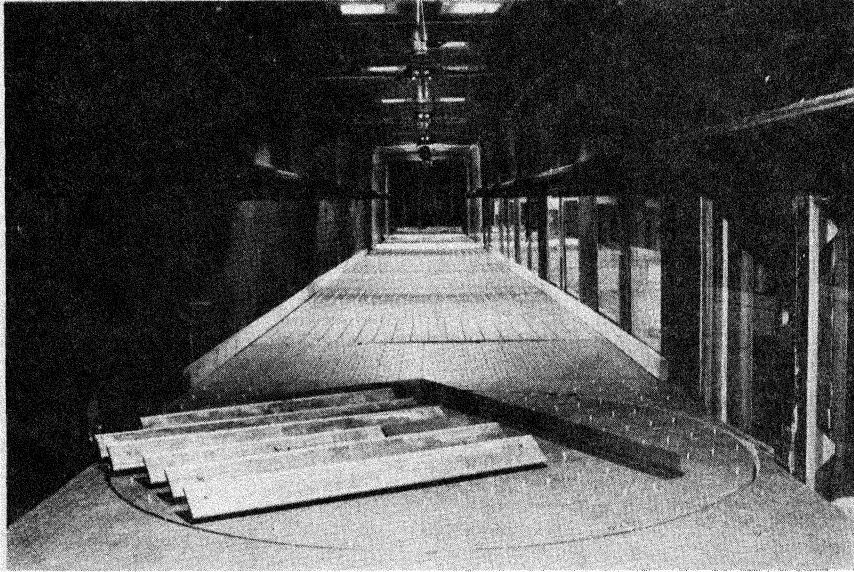


Figure 1. A view of the array field model and fence in the Meteorological Wind Tunnel (configuration NFA4).

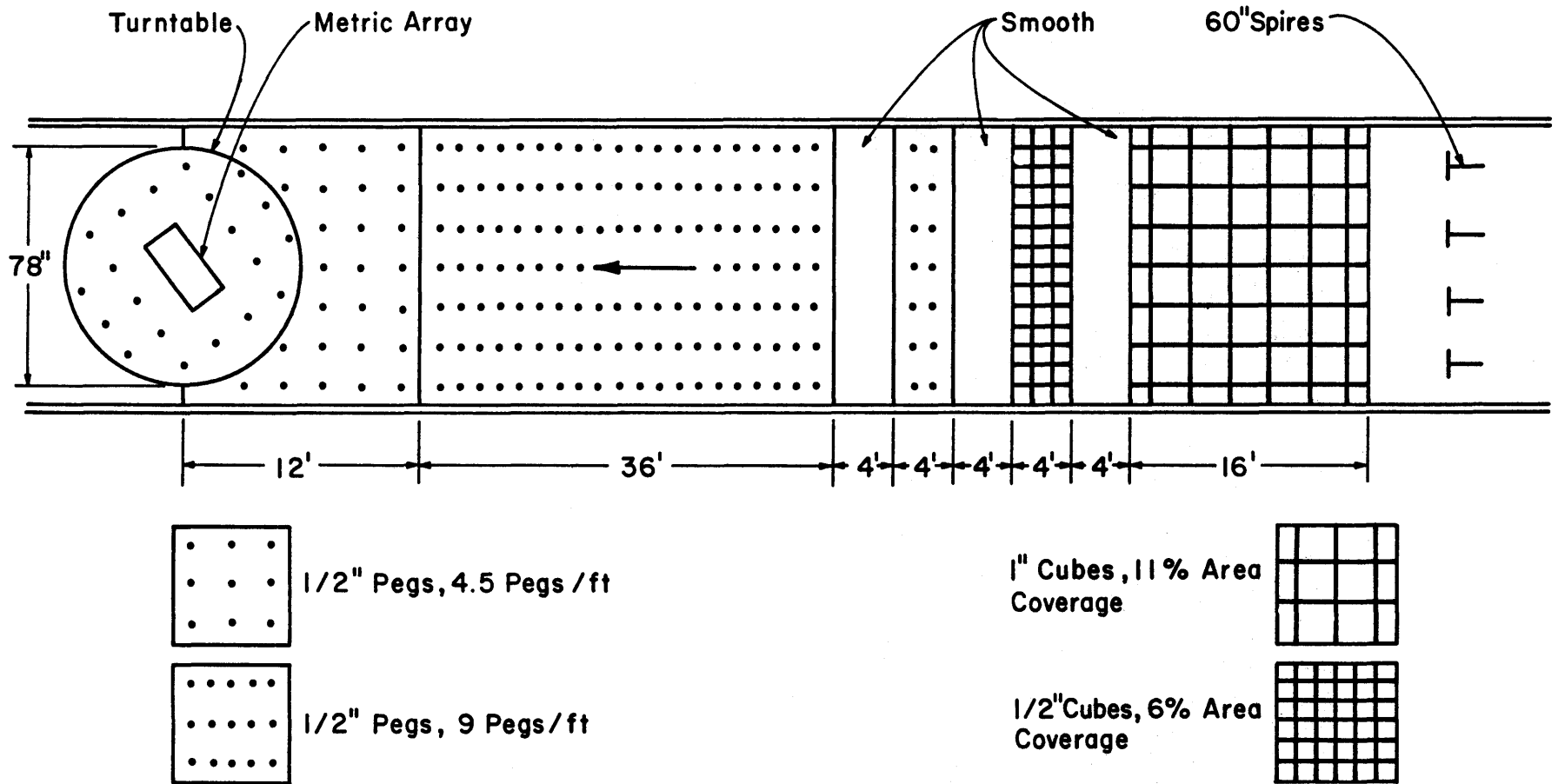


Figure 2. Roughness configuration in the Meteorological Wind Tunnel for generating a  $1/7$  power law (NEWBYL) near the metric array.

## LOG-LOG PROFILE PLOTS

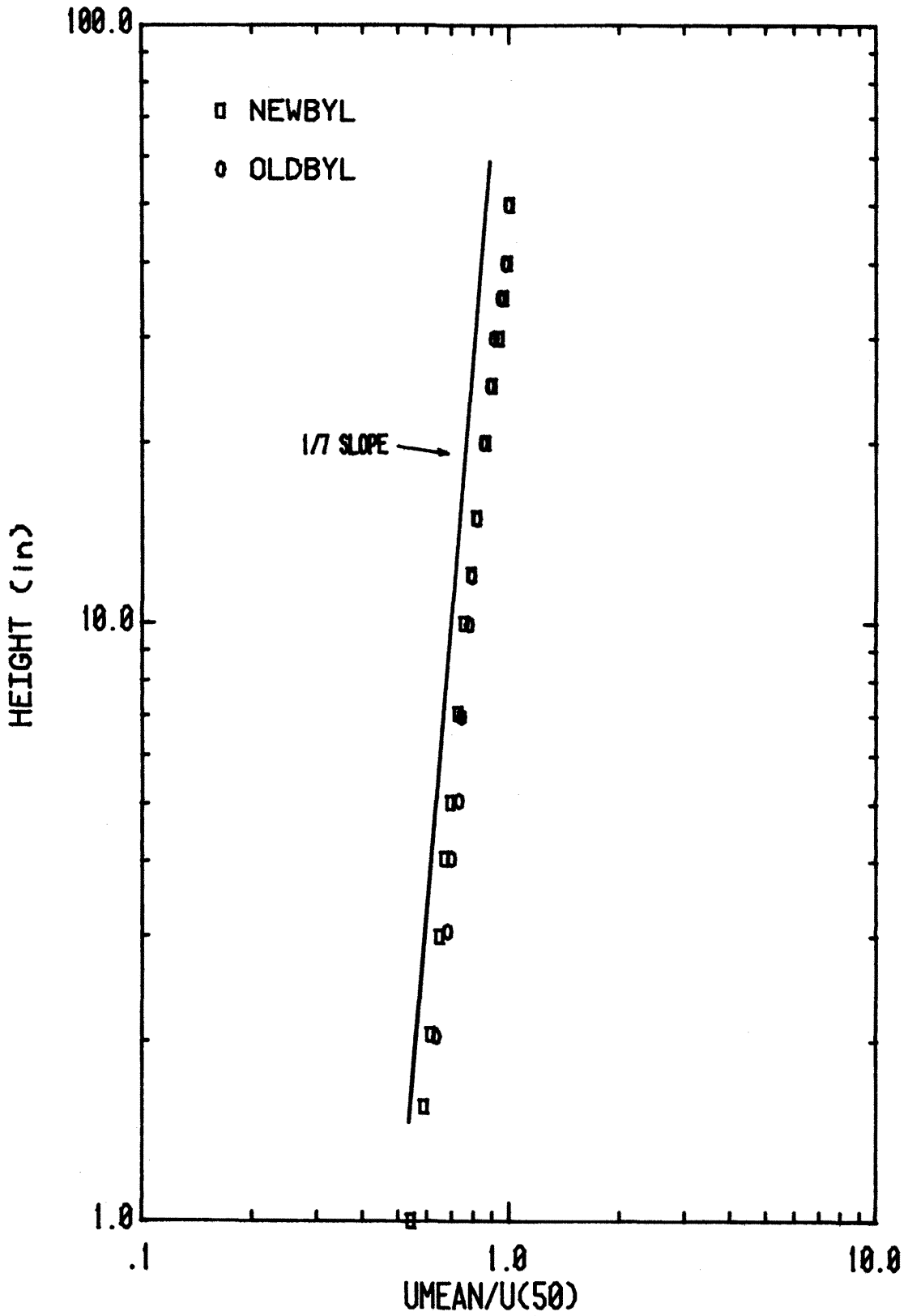


Figure 3. Velocity distribution in the test section.

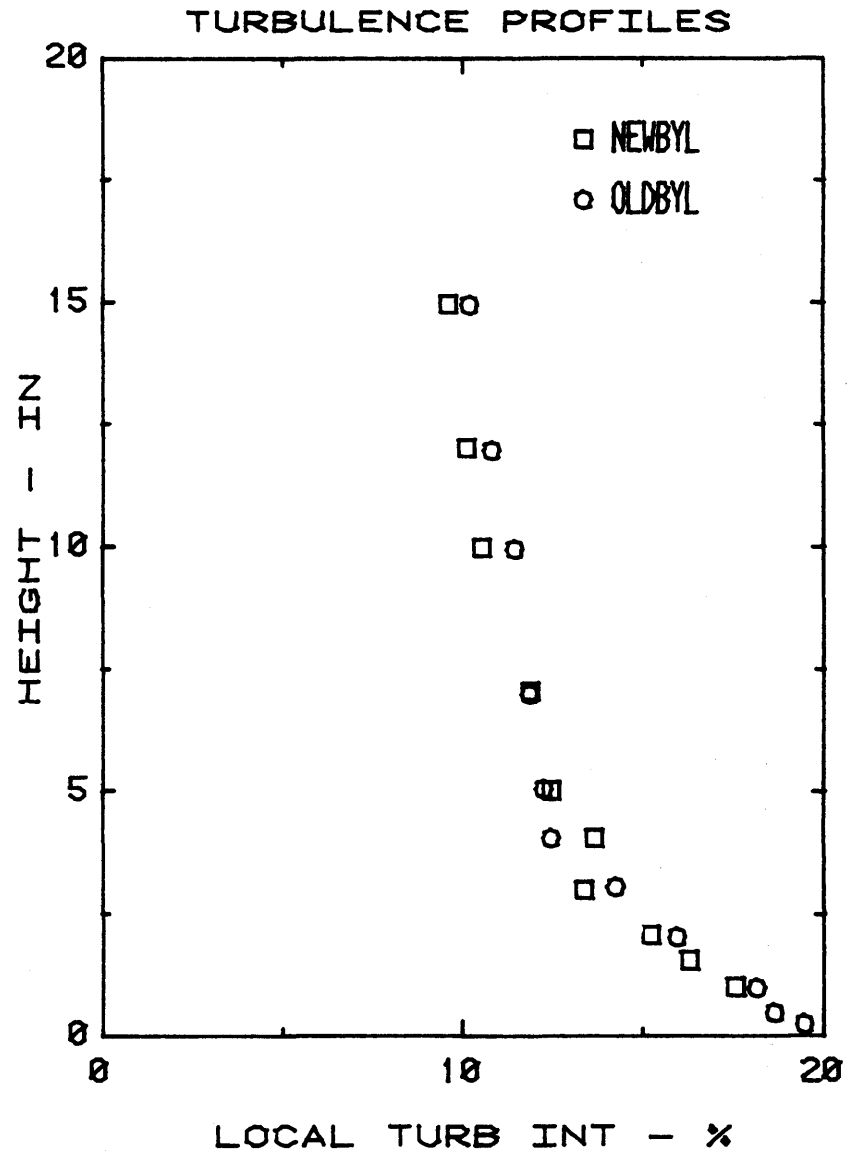
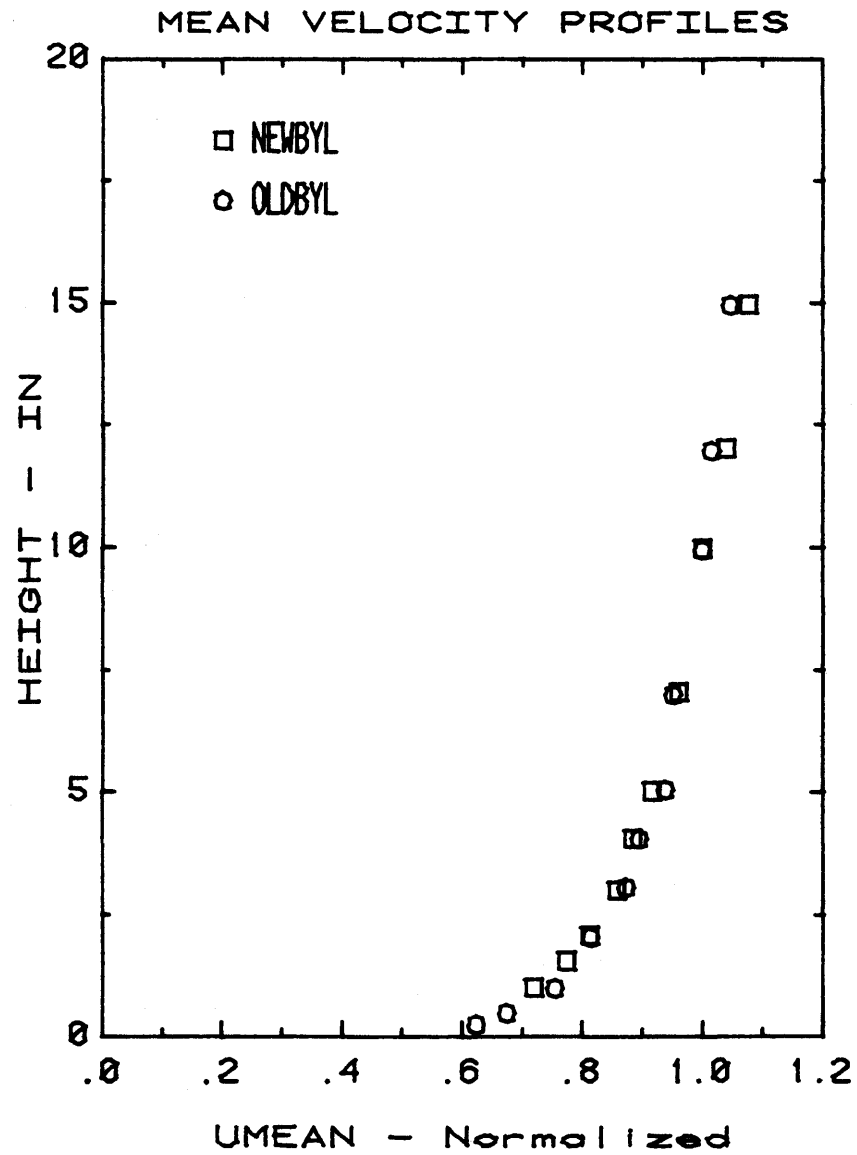


Figure 4. Mean velocities and turbulent intensities in the lower section of the boundary layer.

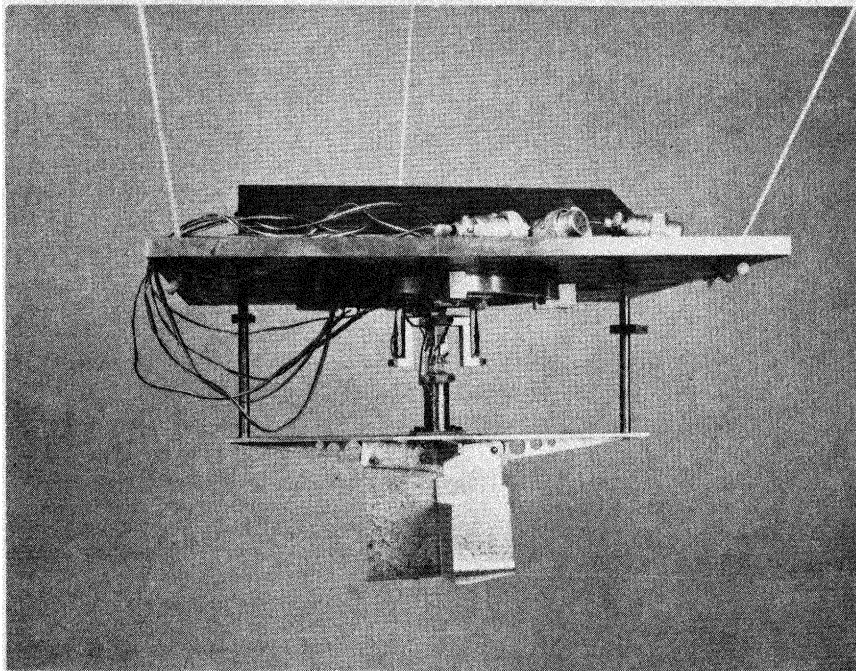
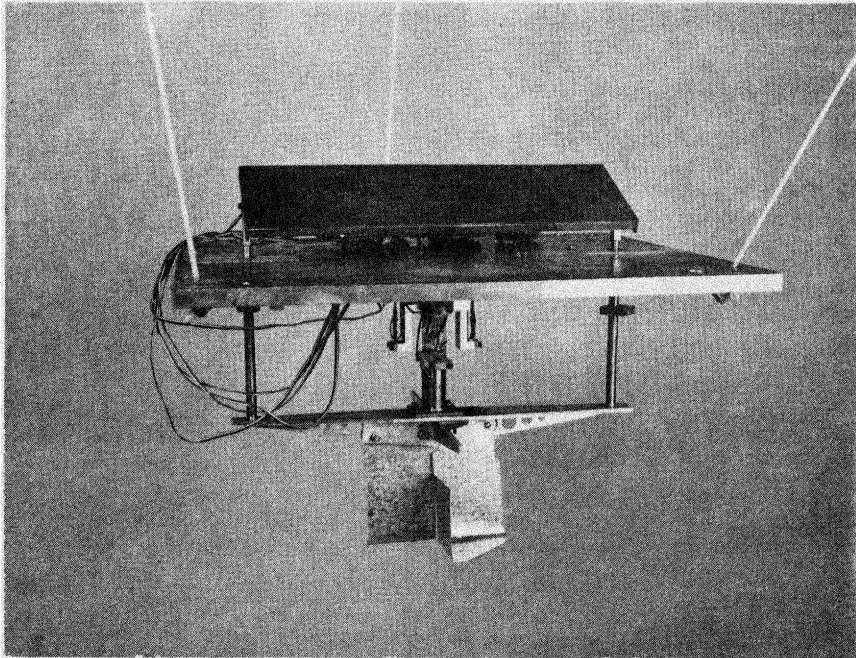


Figure 5. A view of the 6-component balance system and the 1:24 scale model.

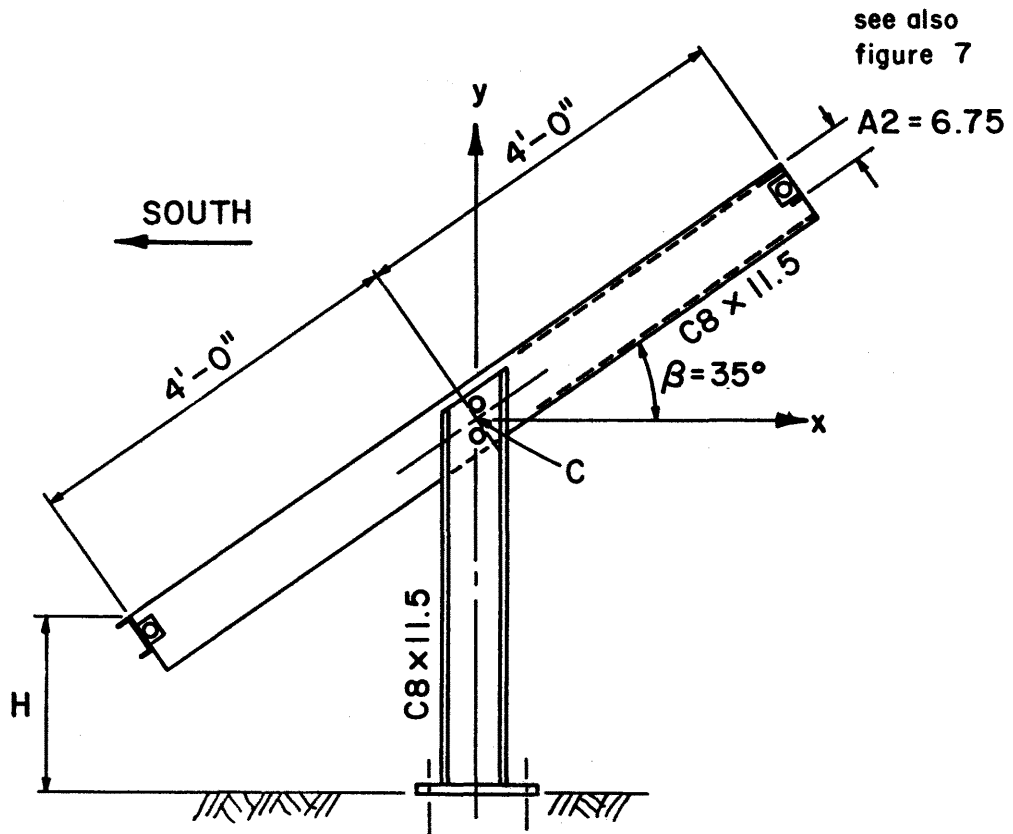
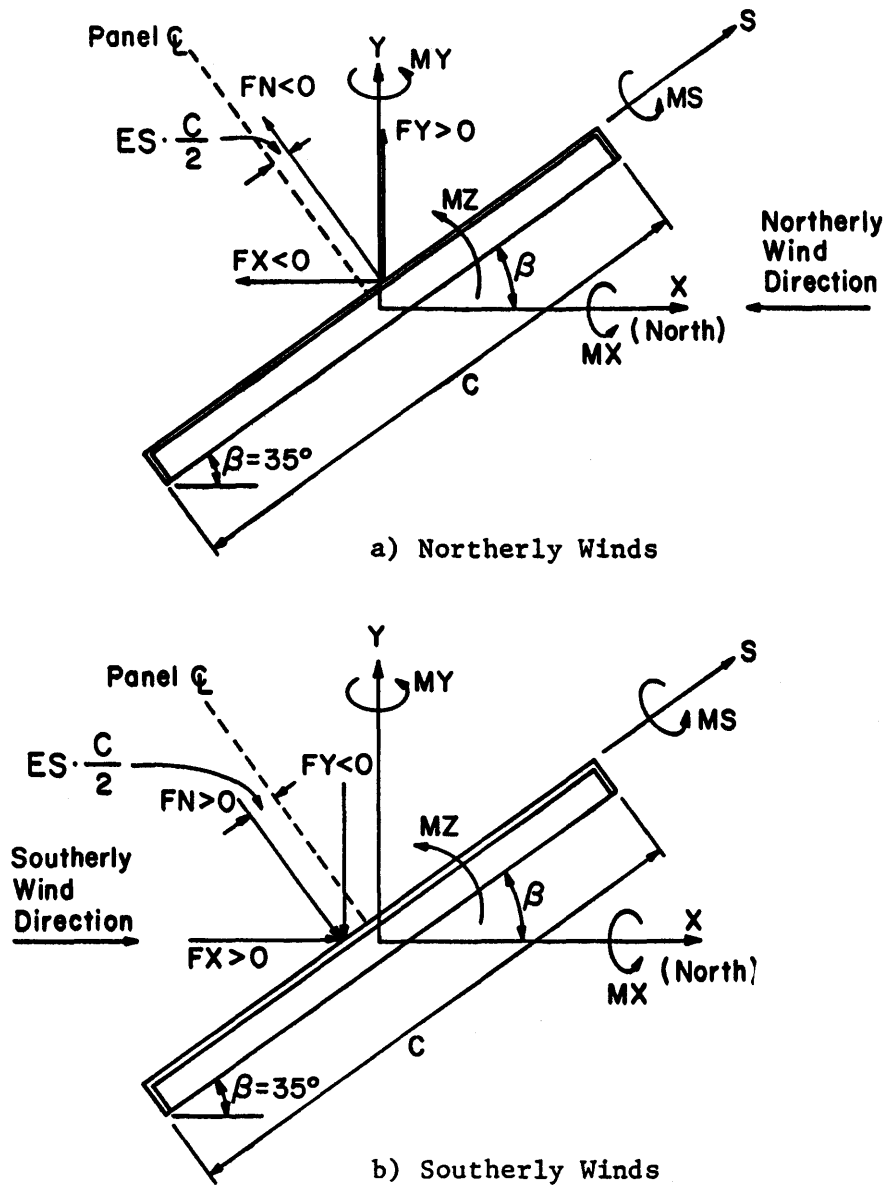


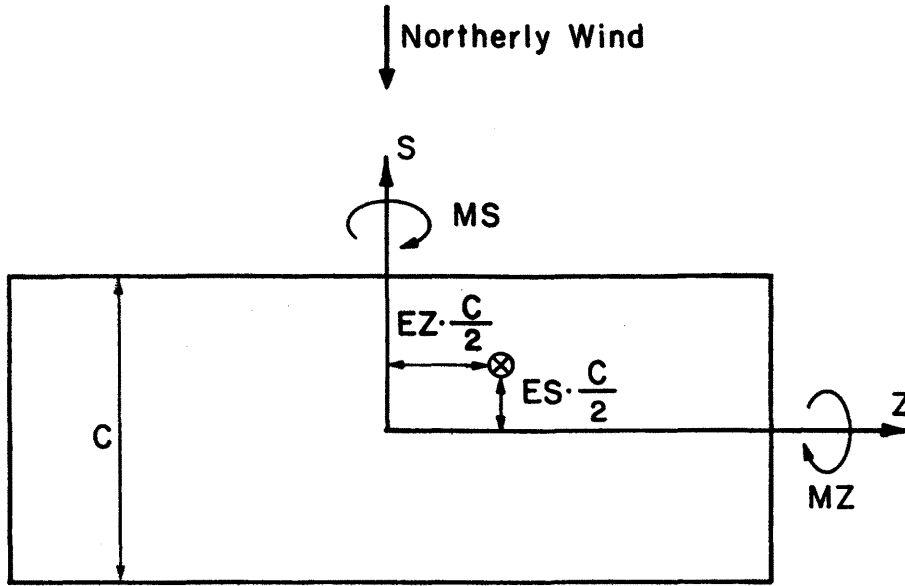
Figure 6. Conceptual low-cost support for a photovoltaic array.



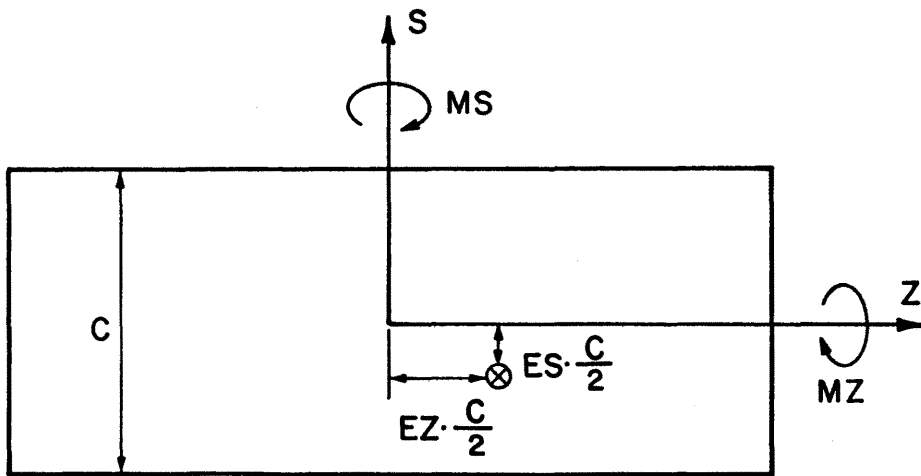


## ELEVATION

Figure 7. Directions of forces and moments for northerly and southerly winds.



a) Northerly Winds



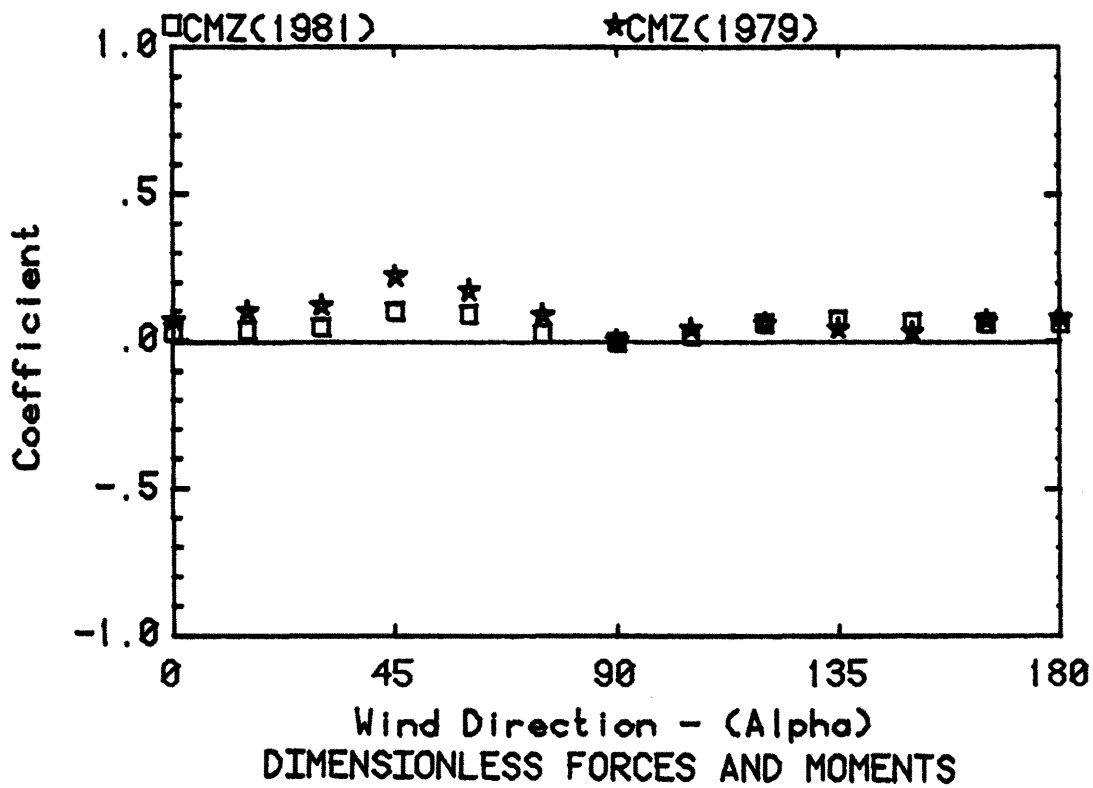
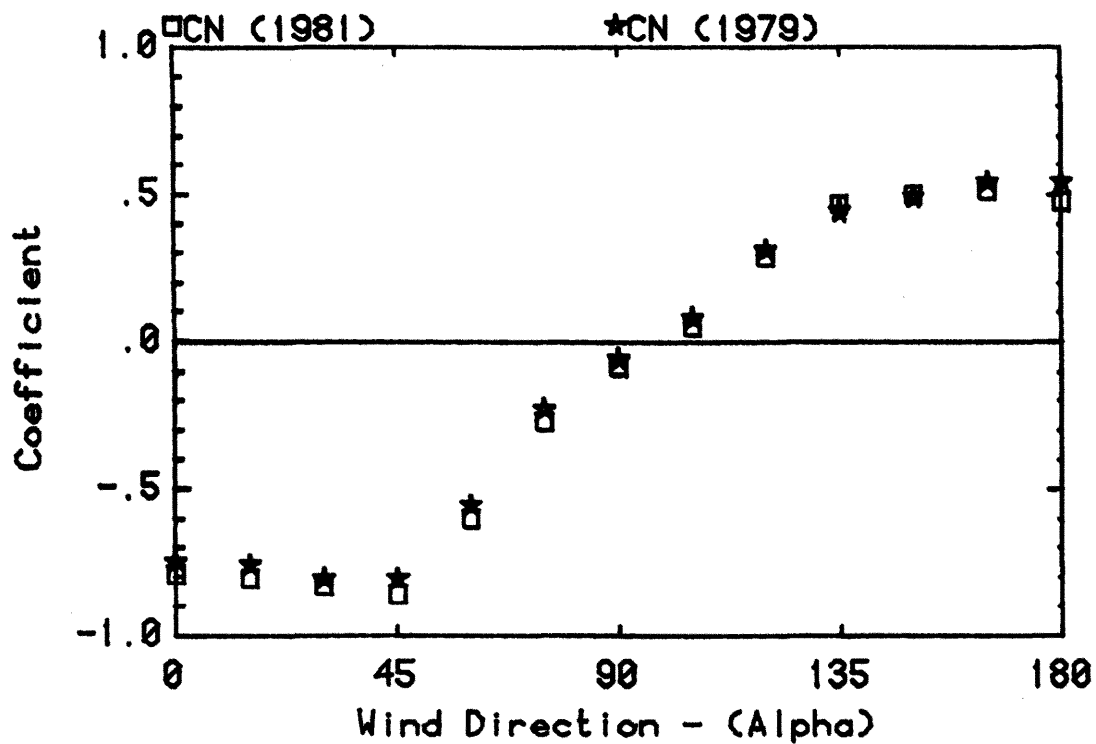
b) Southerly Winds

↑ Southerly Wind

⊗ Action Point of the Normal Force FN

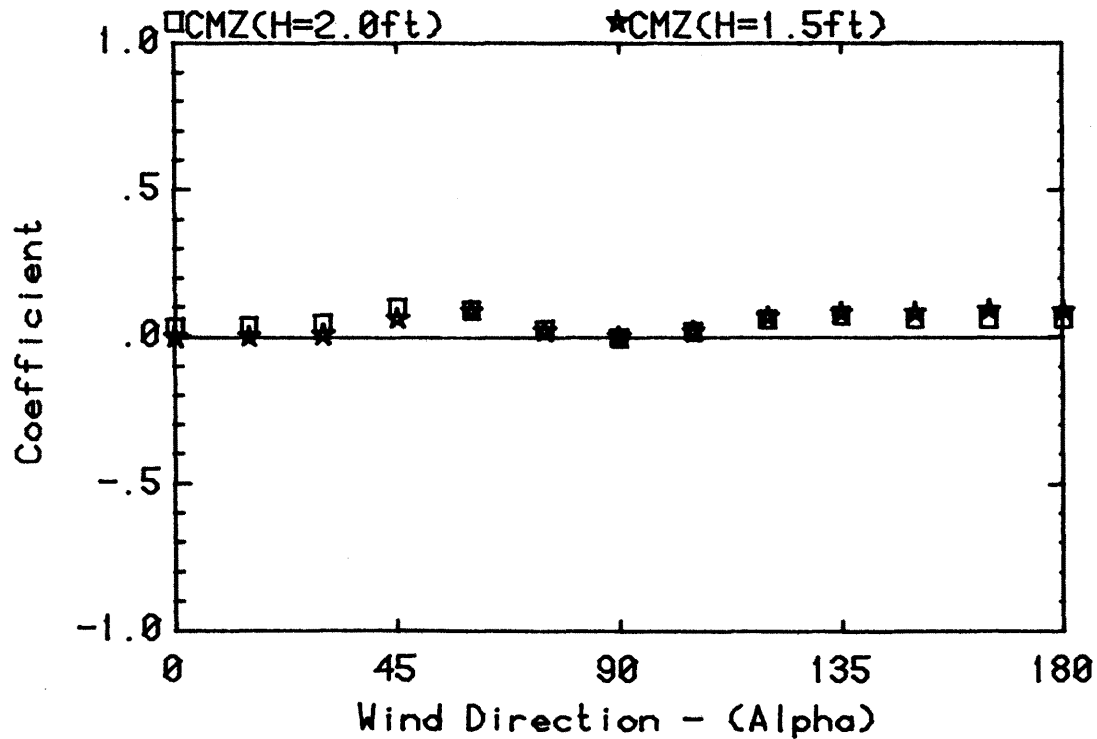
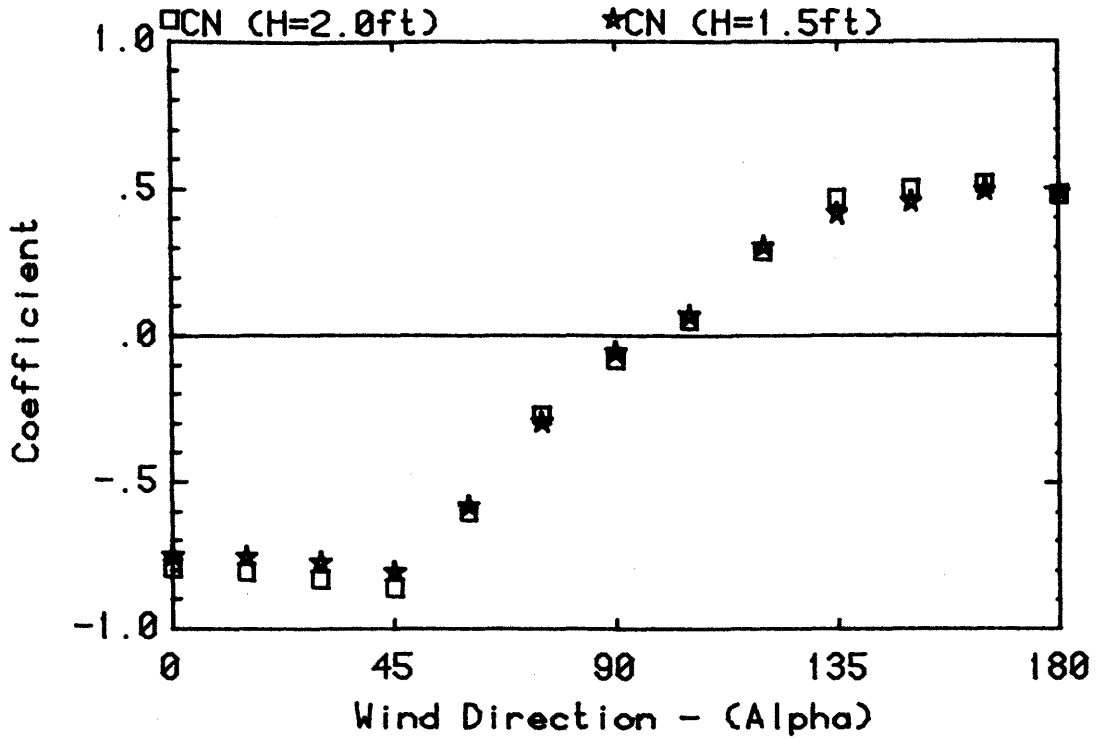
PLAN

Figure 7 (continued).



Single Collector, Beta = 35

Figure 8. The values of CN and CMZ in the present and the previous study (1979), H = 2.0 ft.



DIMENSIONLESS FORCES AND MOMENTS

Single Collector, Beta = 35

Figure 9. The values of CN and CMZ for H = 2.0 ft and H = 1.5 ft.

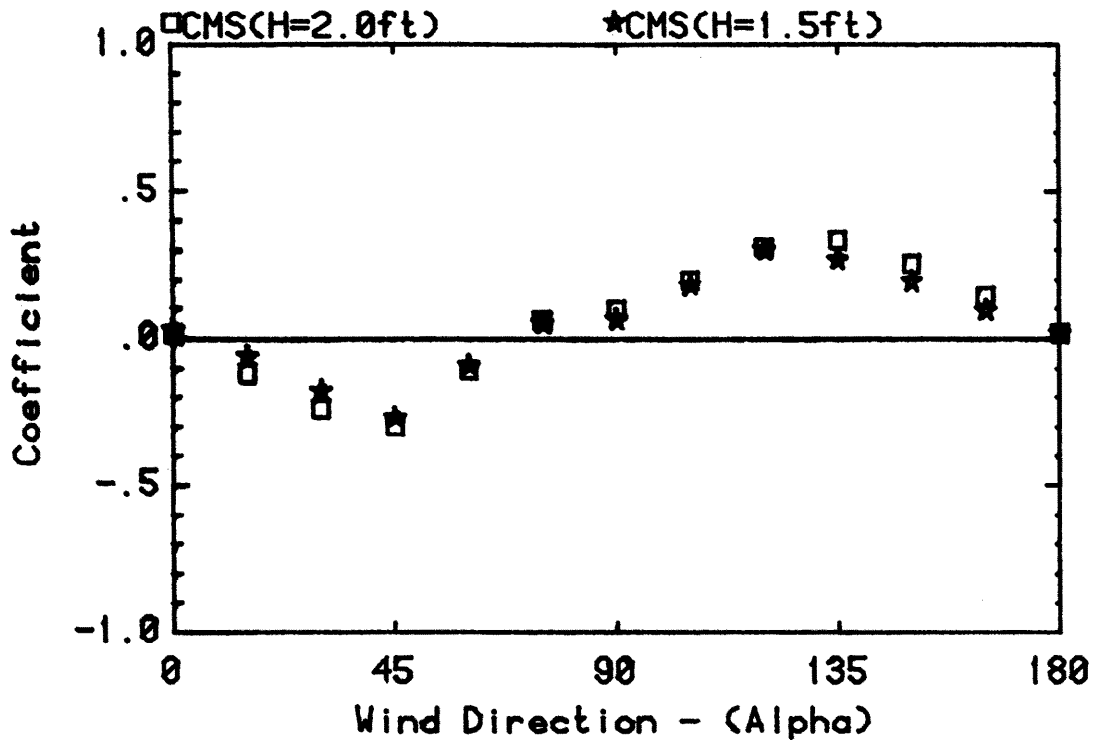


Figure 10. The values of CMS for H = 2.0 ft and H = 1.5 ft.

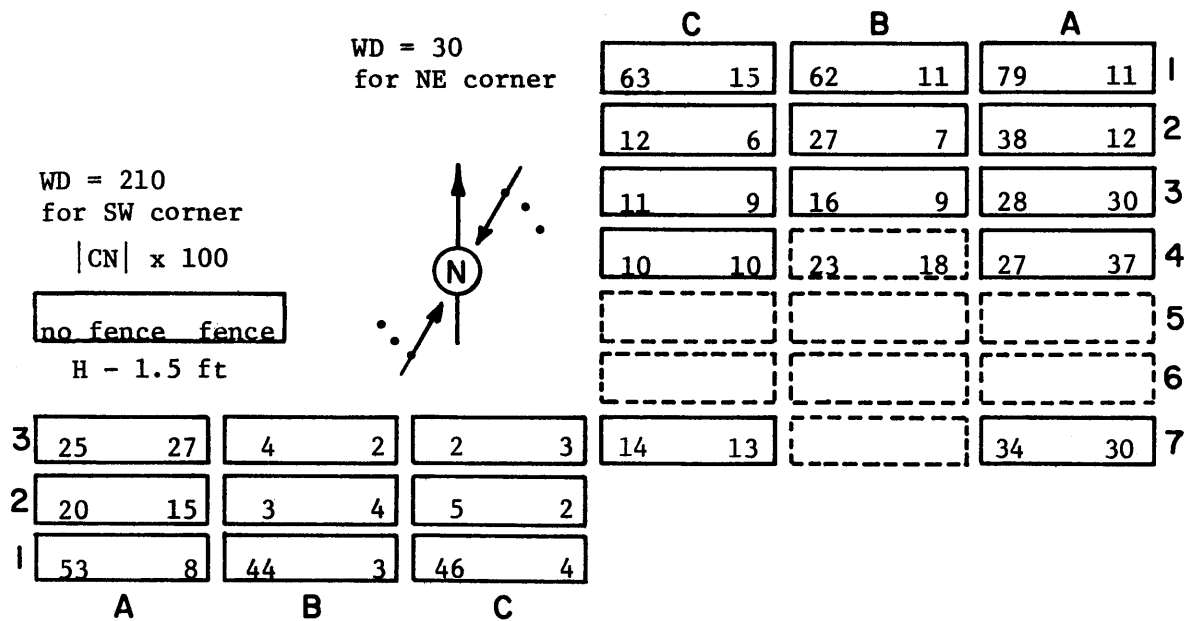
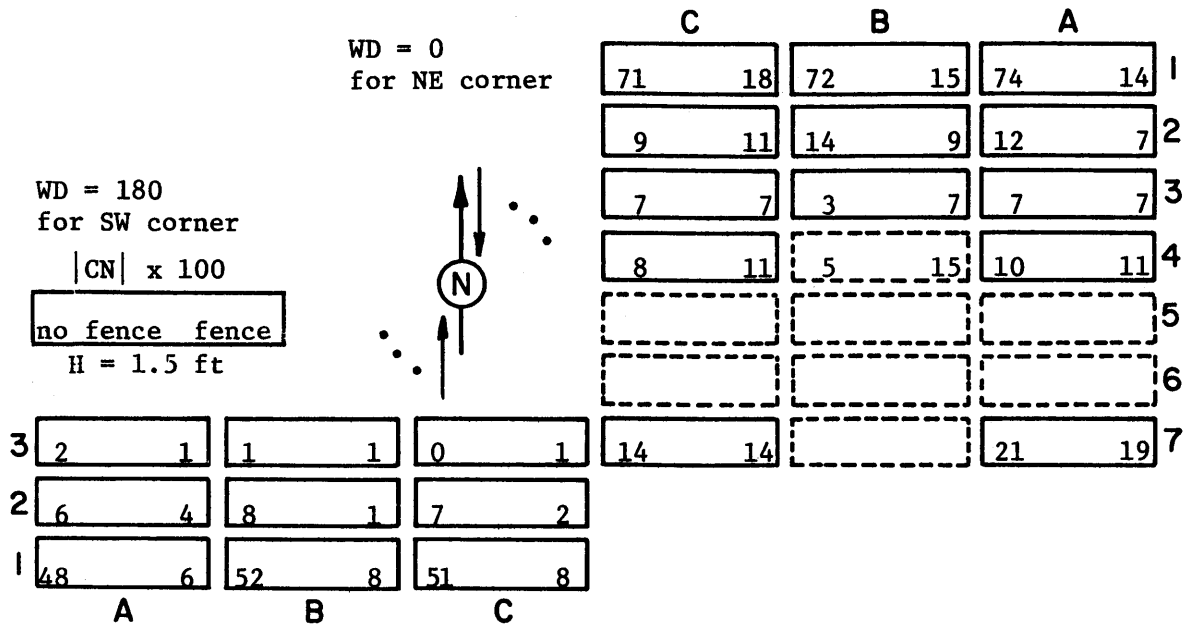


Figure 11. Distribution of |CN| x 100 in the field (left number, without fence; right number, with fence).

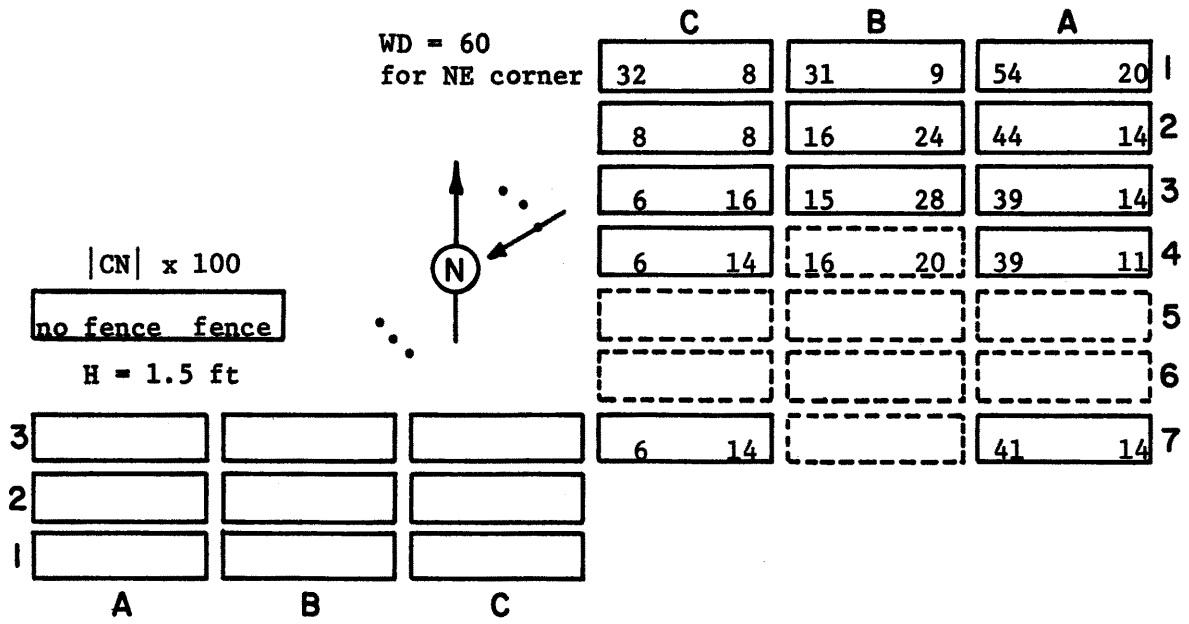
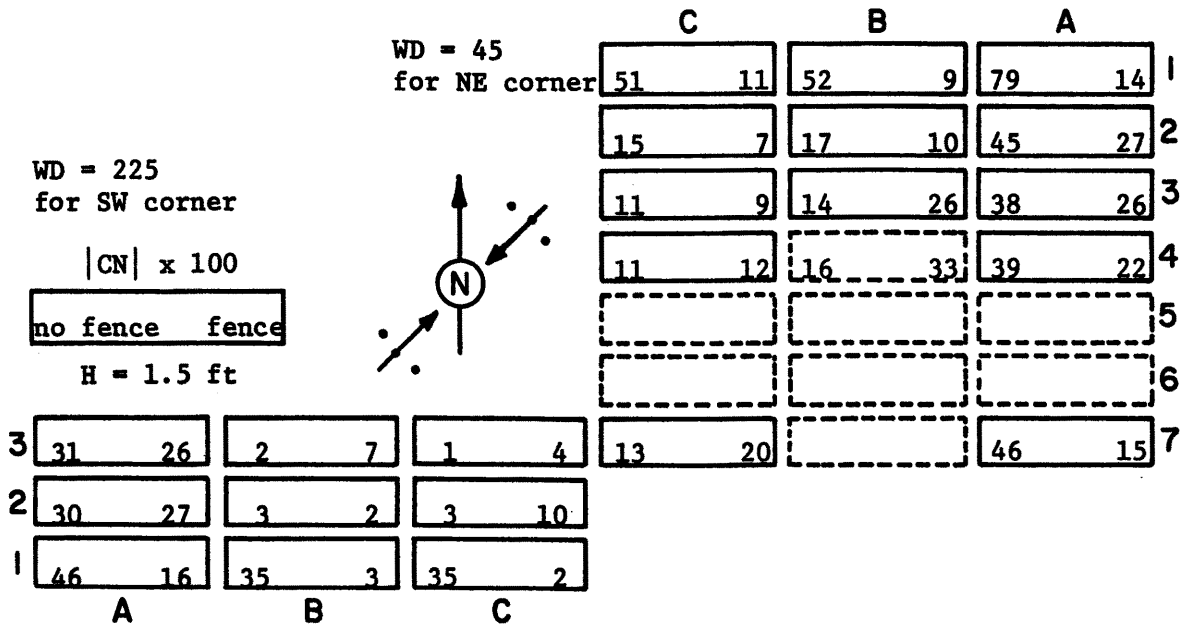
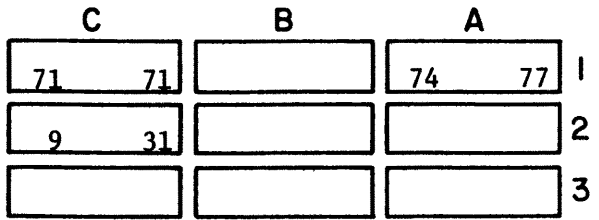
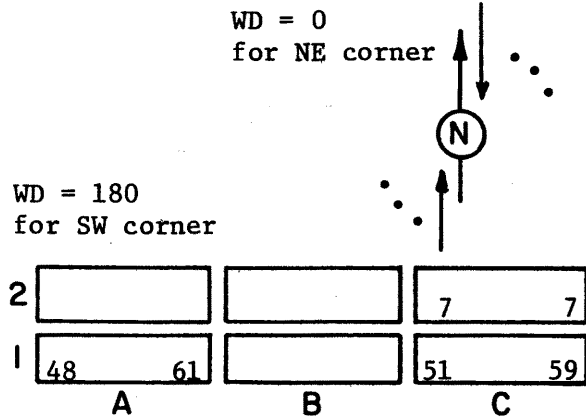
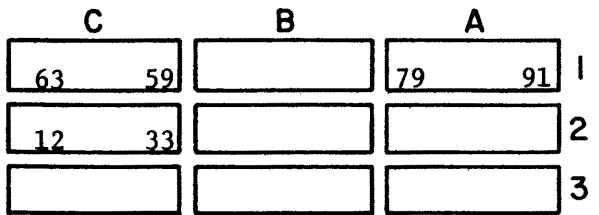
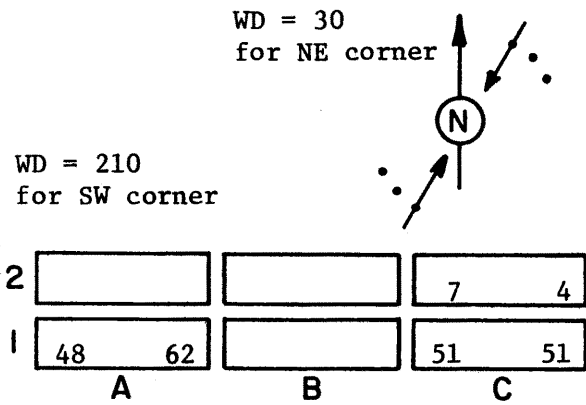


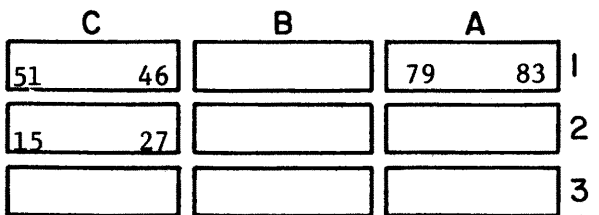
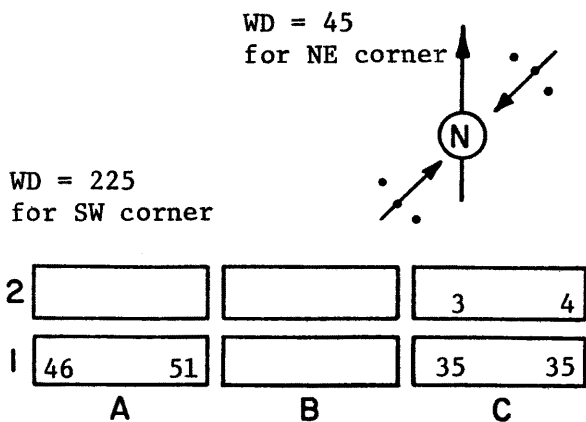
Figure 11 (continued).



$|CN| \times 100$   
 $H = \boxed{1.5 \quad 2.0} \text{ ft}$   
 No fence



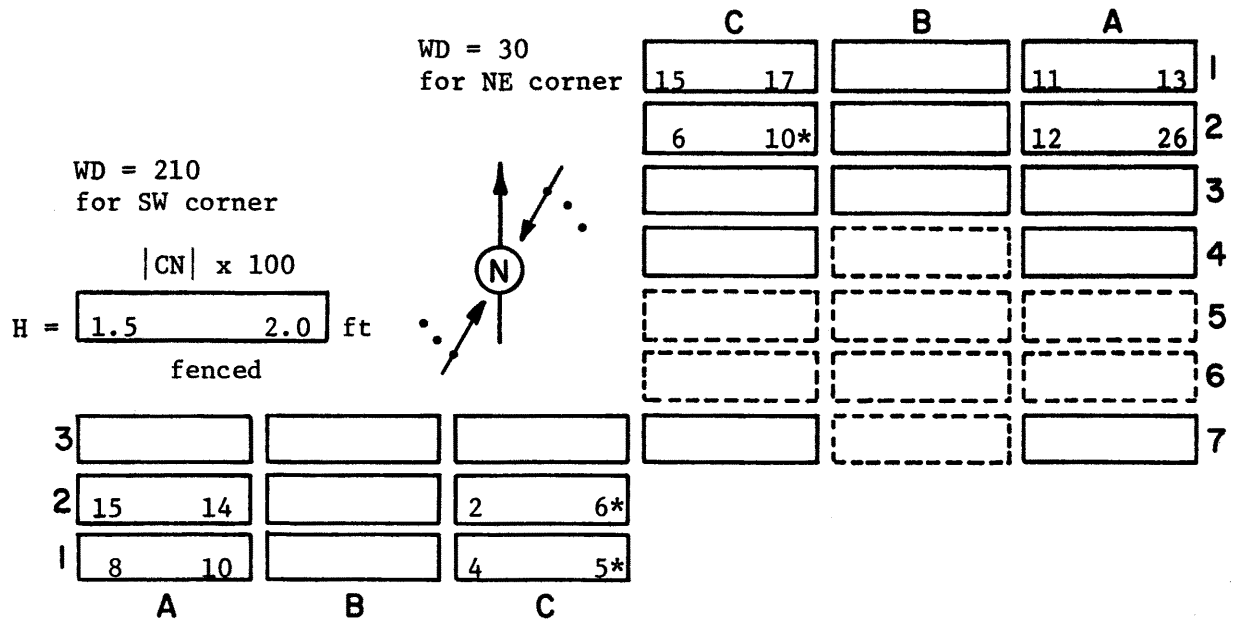
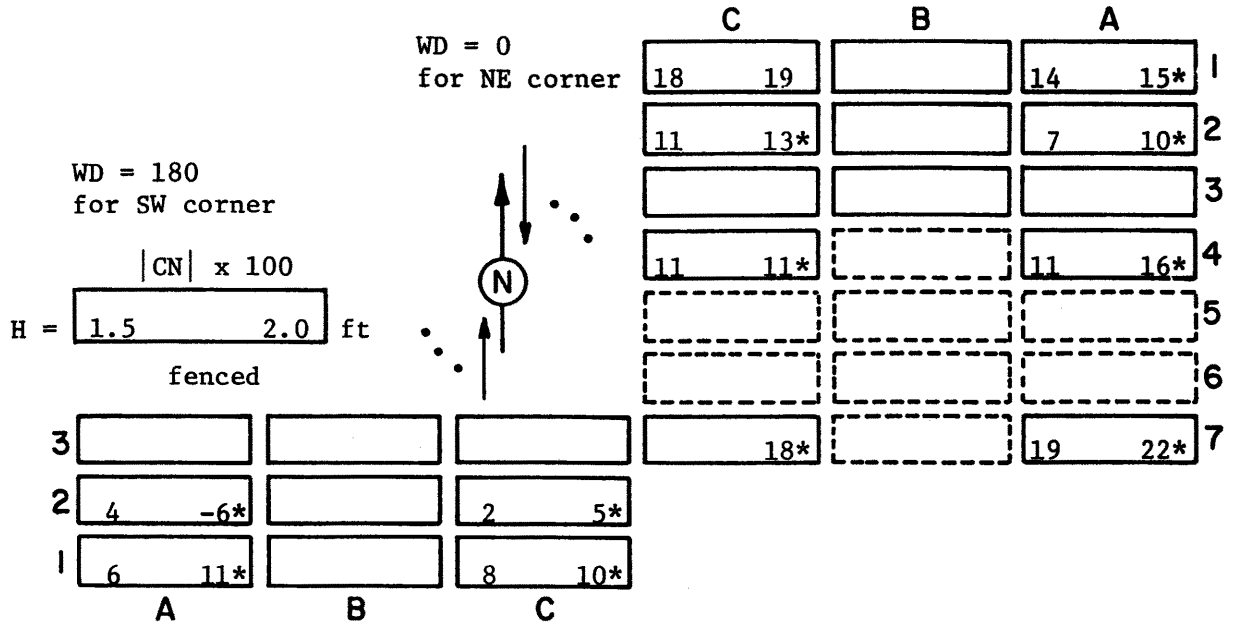
$|CN| \times 100$   
 $H = \boxed{1.5 \quad 2.0} \text{ ft}$



$|CN| \times 100$   
 $H = \boxed{1.5 \quad 2.0} \text{ ft}$

Figure 12. Comparison of values of  $|CN| \times 100$  for  $H = 1.5 \text{ ft}$  (left) and  $H = 2.0 \text{ ft}$  (right) without a fence.





\*Denotes a fence without a corner modification

Figure 13. Comparison of values of  $|CN| \times 100$  for fenced fields with  $H = 1.5 \text{ ft}$  (left) and  $H = 2.0 \text{ ft}$  (right).

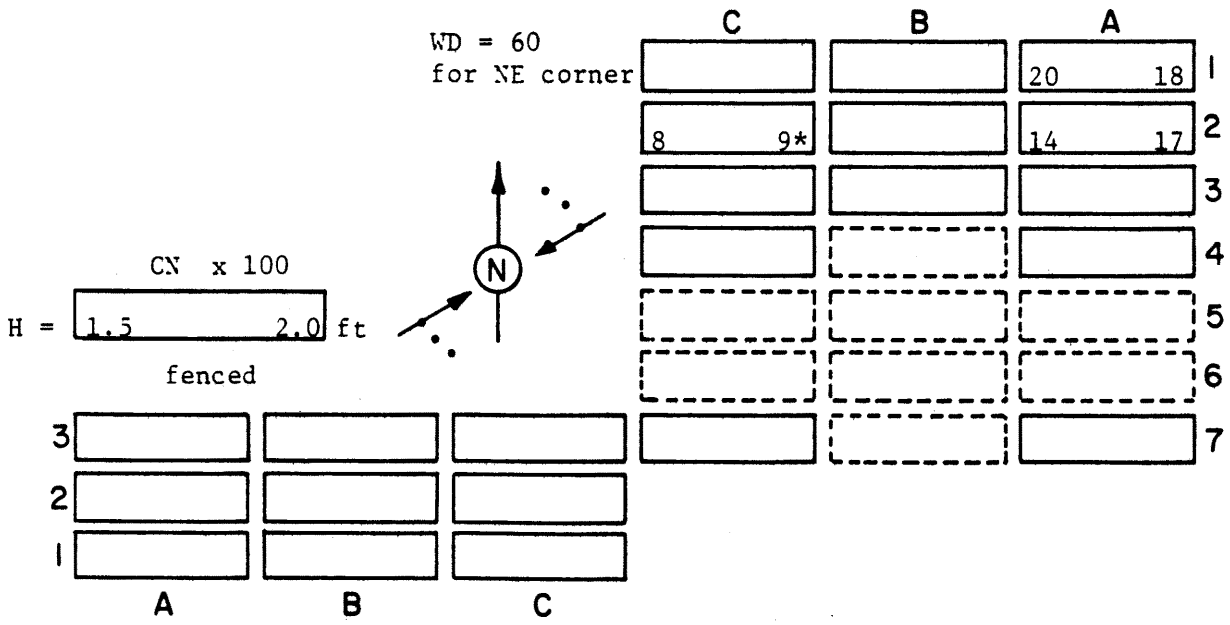
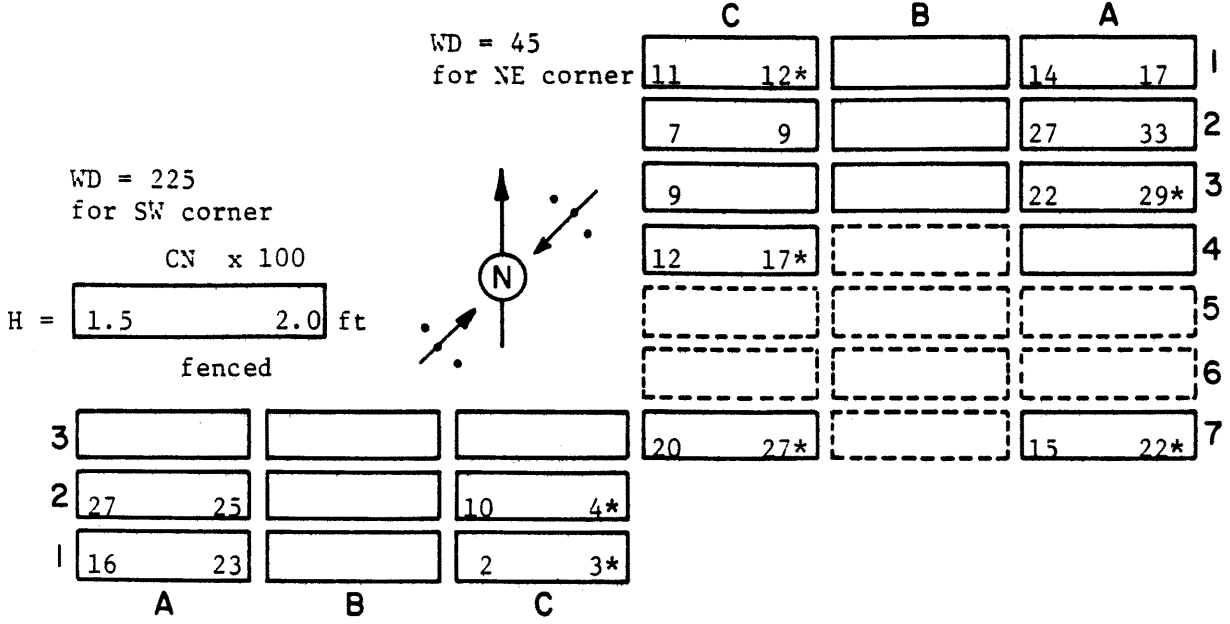


Figure 13 (continued).

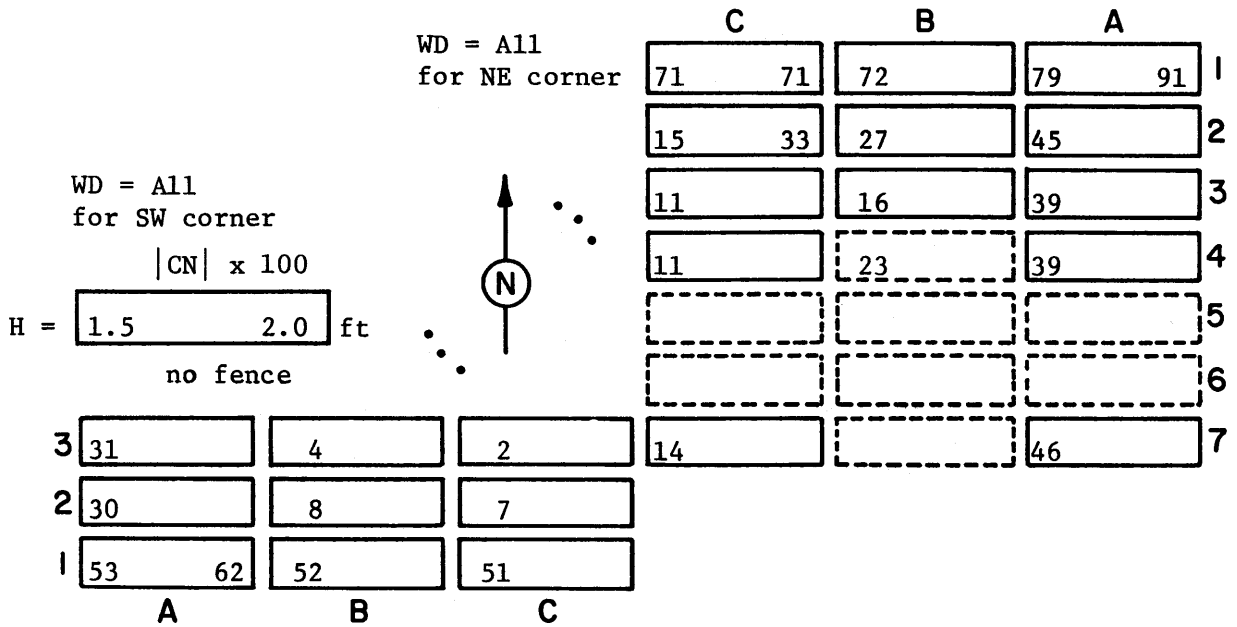


Figure 14. Maximum values of  $|CN| \times 100$  without a fence for all wind directions for  $H = 1.5$  ft (left) and  $H = 2.0$  ft (right).

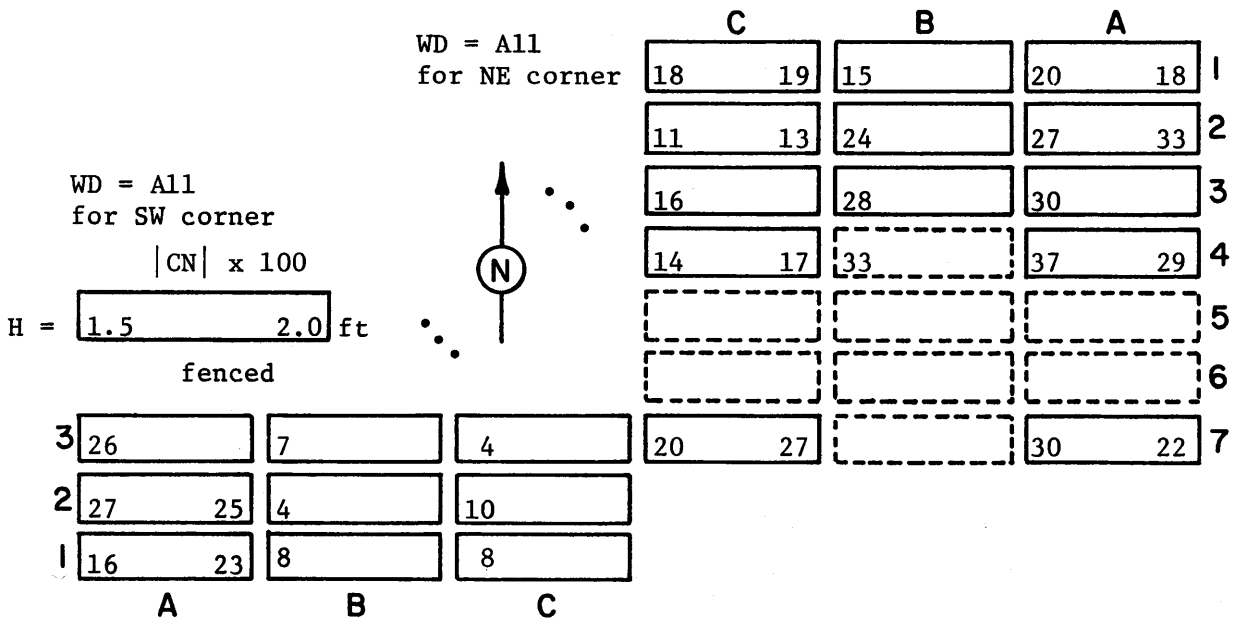


Figure 15. Maximum values of  $|CN| \times 100$  with a fence (and a corner fence) for all wind directions for  $H = 1.5$  ft (left) and  $H = 2.0$  ft (right).  
Note: Higher values for  $H = 1.5$  ft are usually from the  $WD = 30$  which is missing in the  $H = 2.0$  ft tests.

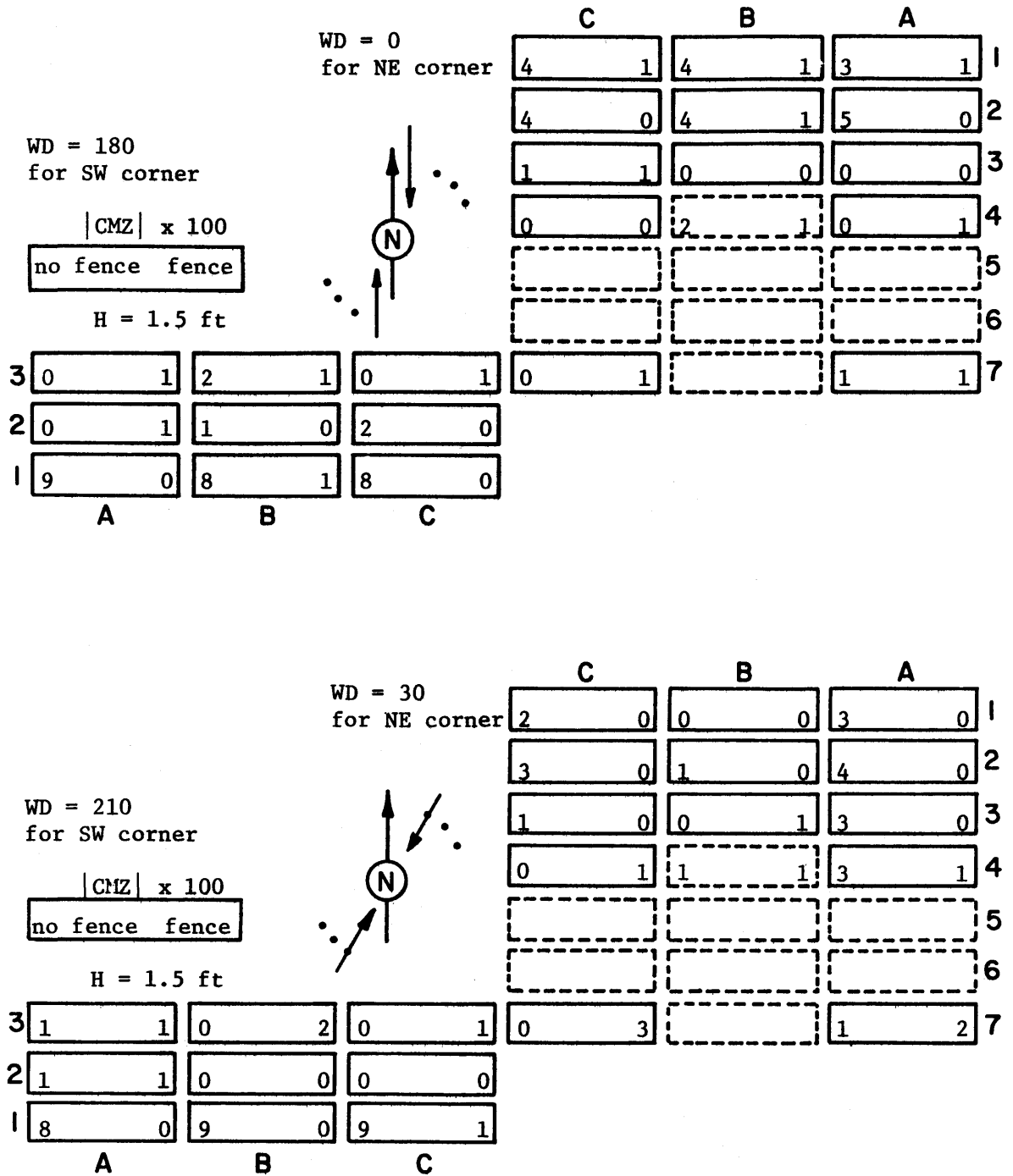


Figure 16. Distribution of  $|CMZ| \times 100$  in the field (left number--without fence, right number--with fence).

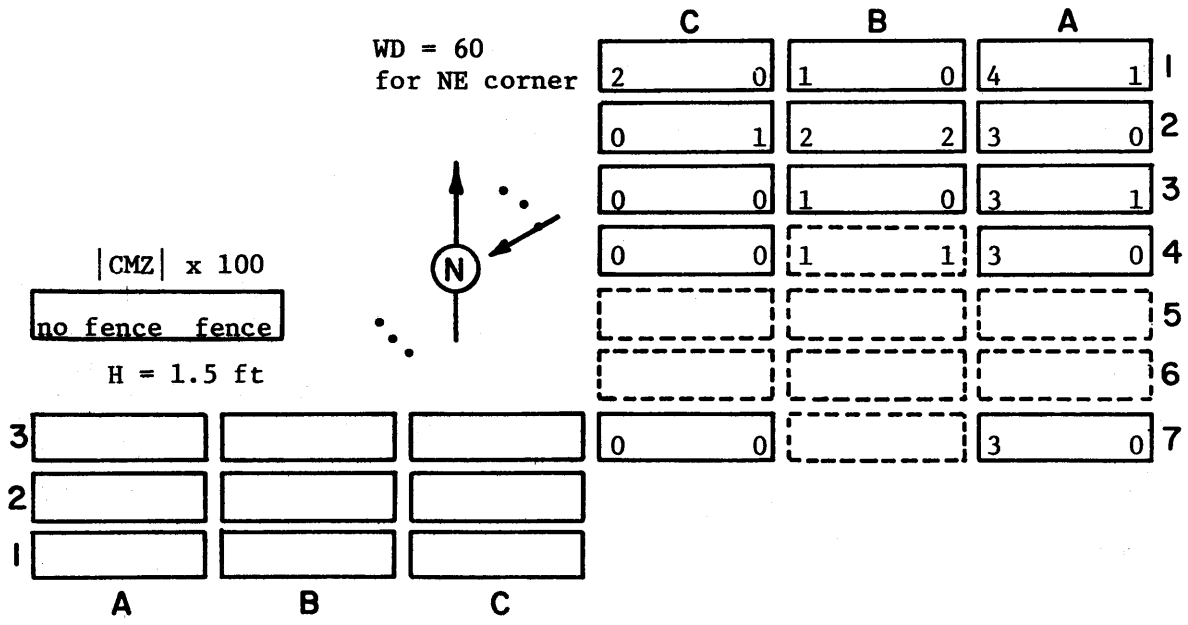
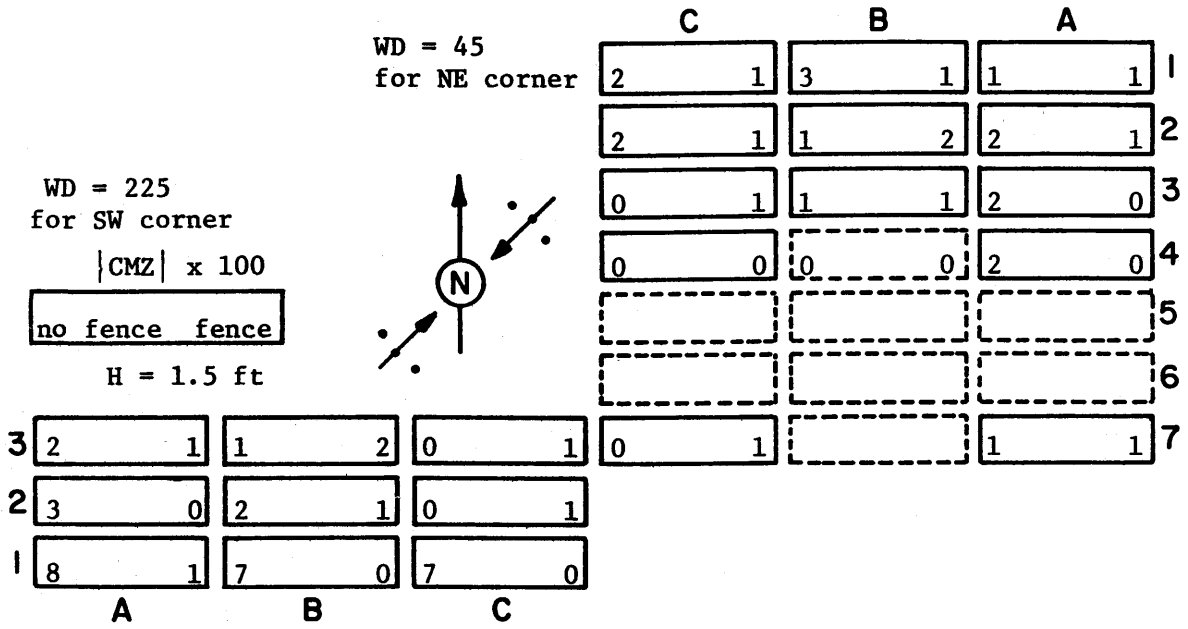


Figure 16 (continued).

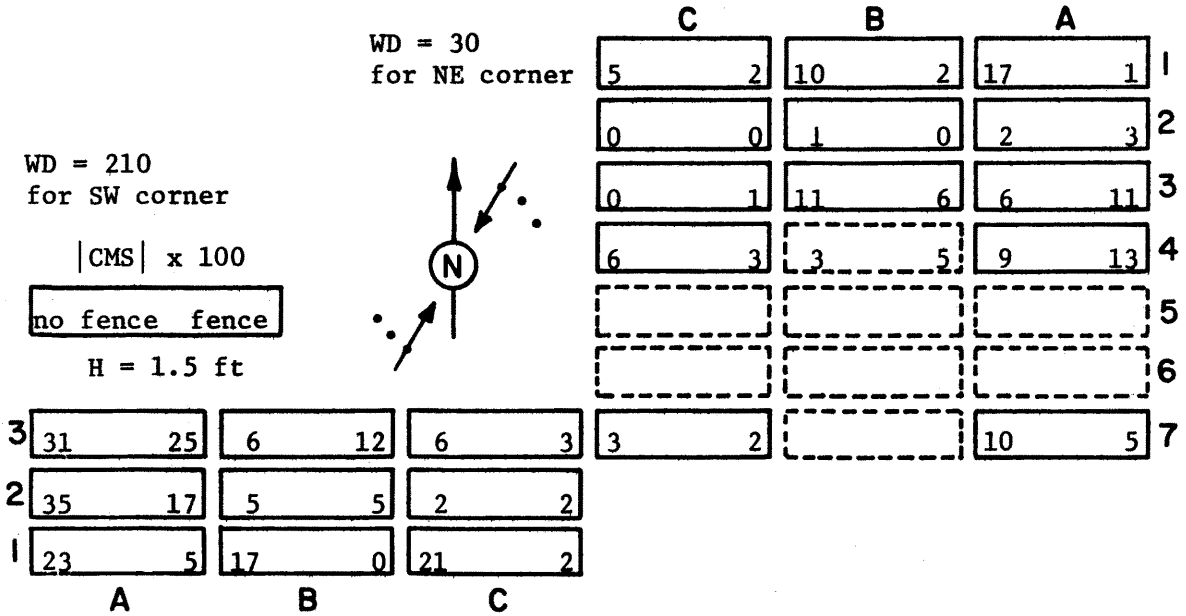
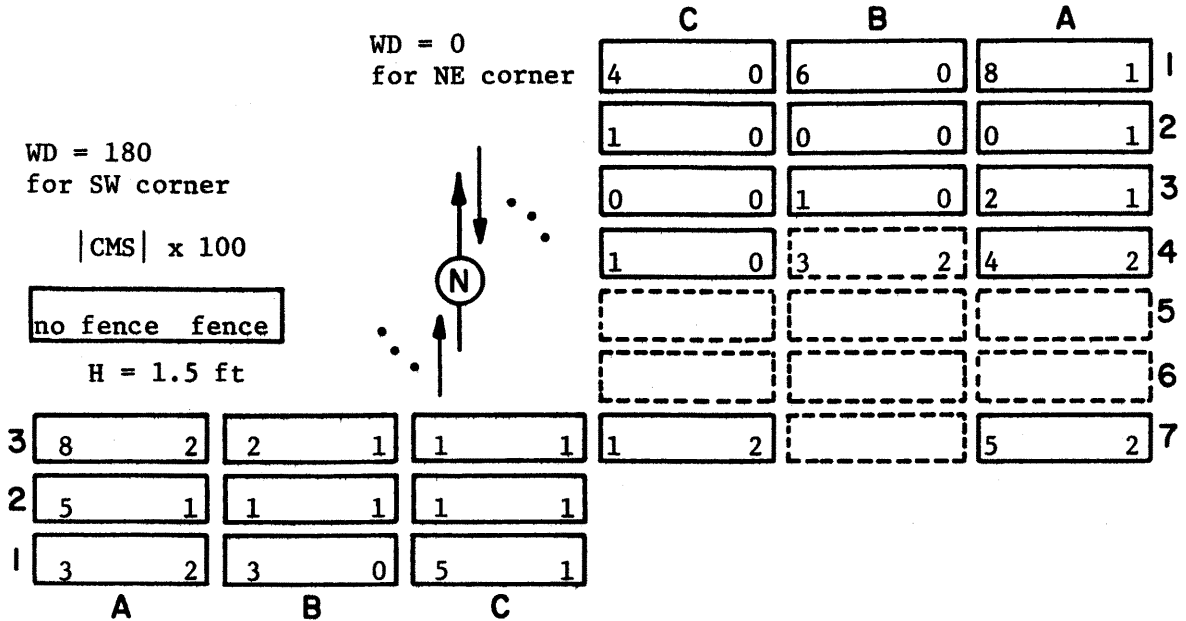


Figure 17. Distribution of  $|CMS| \times 100$  in the field (left number--without fence, right number--with fence).

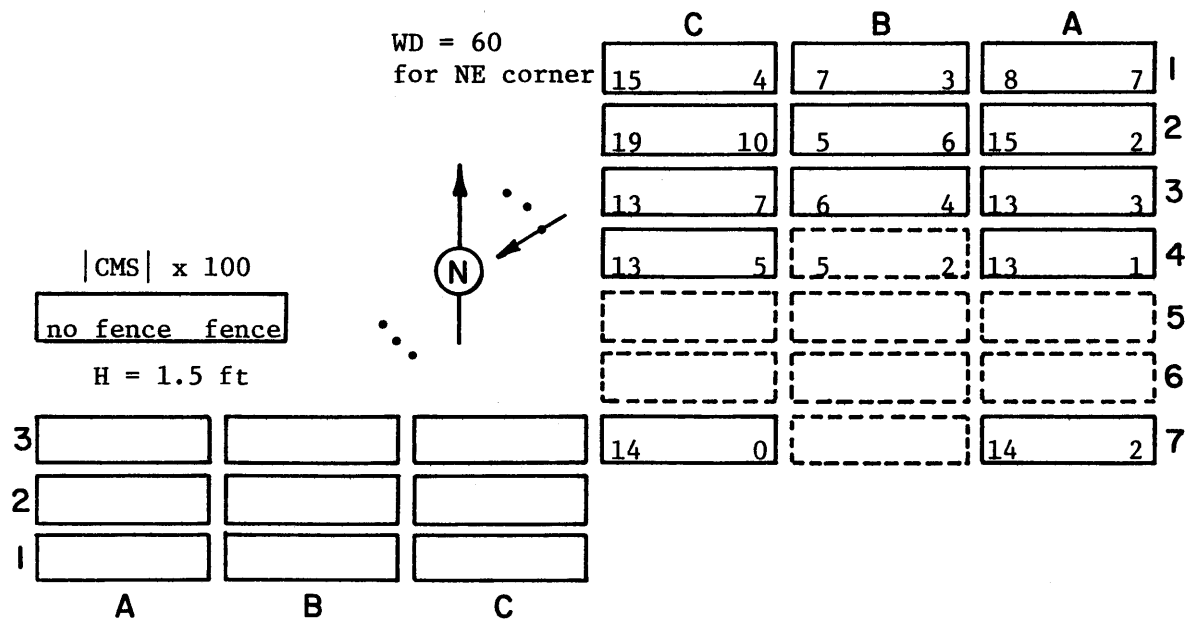
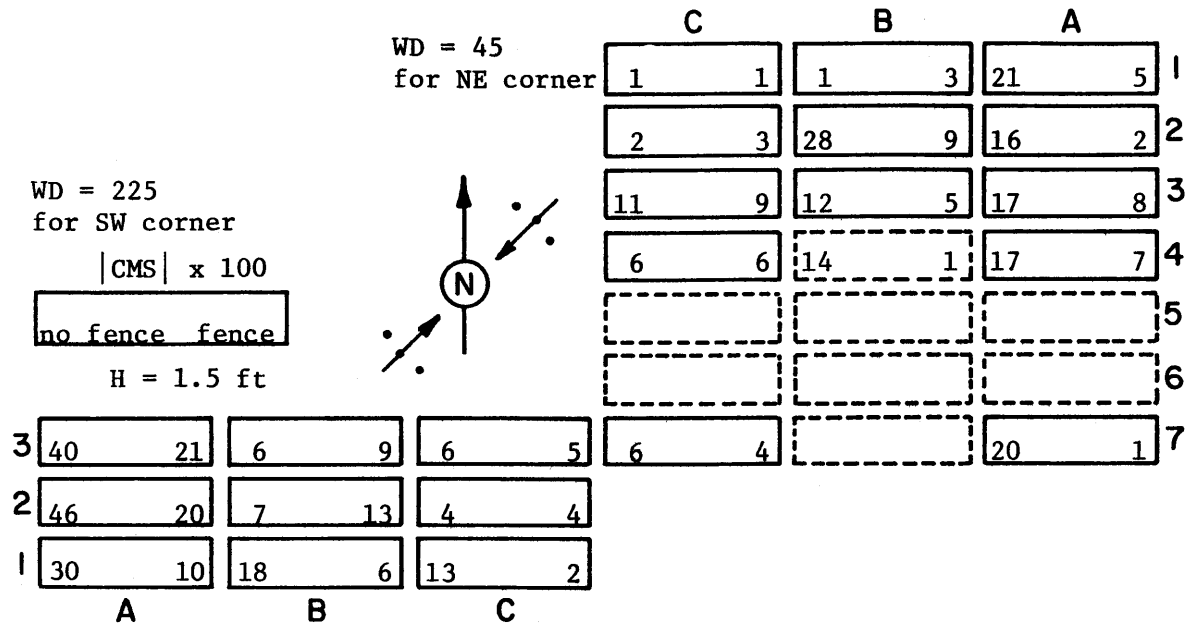
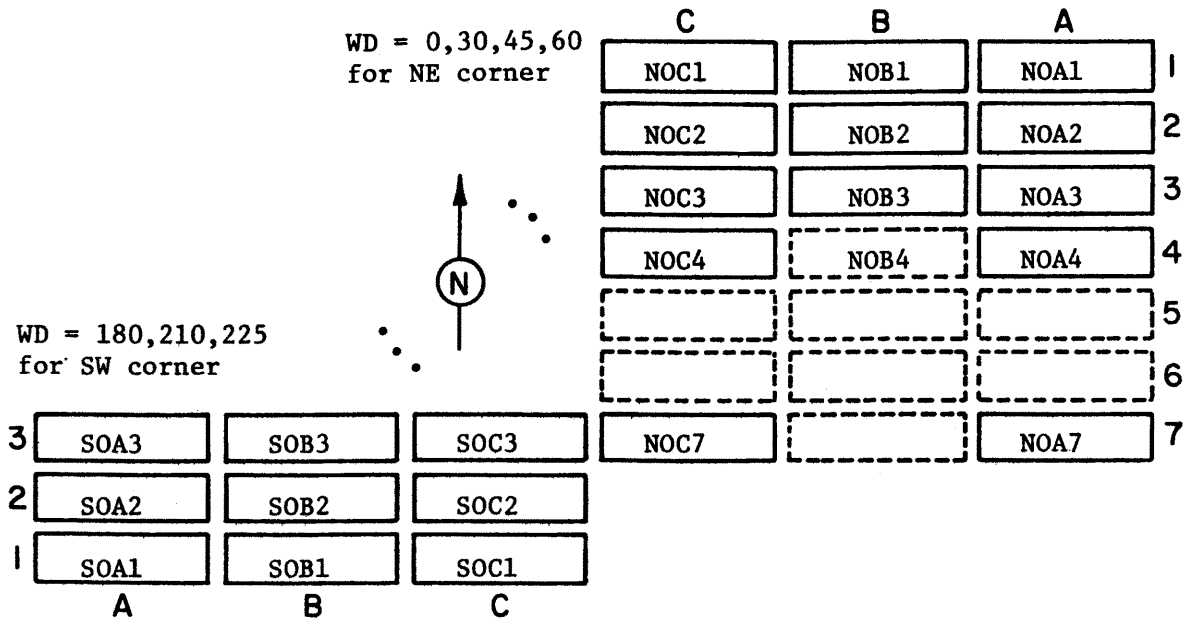
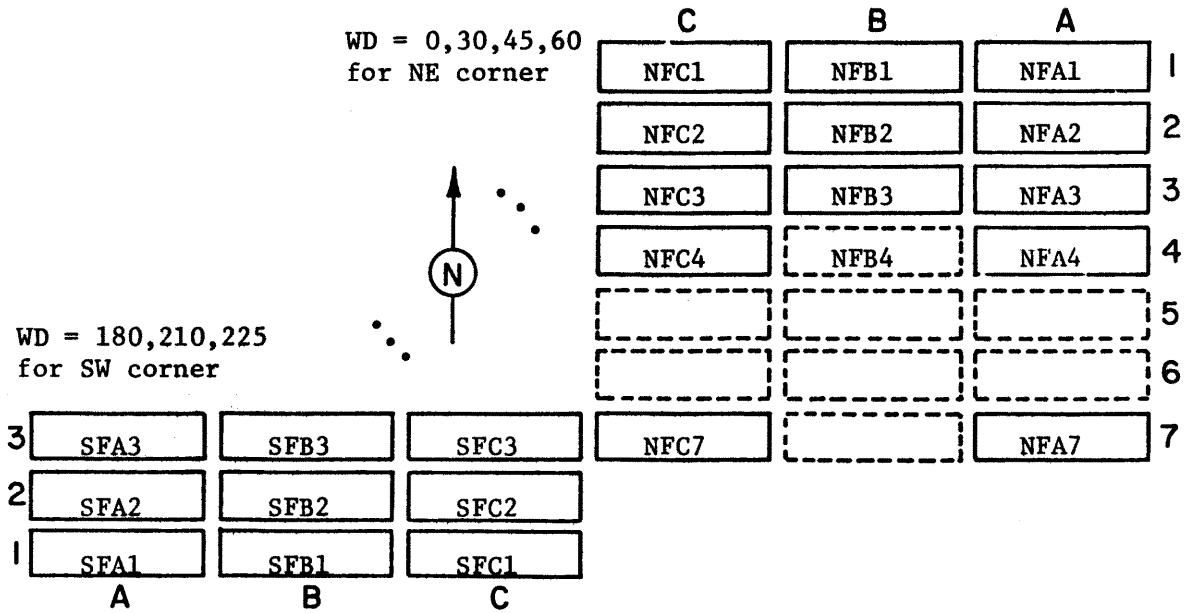


Figure 17 (continued).



Notation for the field with no fence.



Notation for the field with fence.

Figure 18. Notation used for array location and field test files.



## APPENDIX A

AERODYNAMIC COEFFICIENTS FOR  
PHOTOVOLTAIC ARRAYS

H = 1.5 ft

(see Figure 18 for file notation)

and

S20 = Single array at H = 2.0 ft

S15 = Single array at H = 1.5 ft

## DATA FOR FILE : S20

RUN	CONF	WIND	CM	CMZ	ES	CMS	EZ
292	35	0.0	-.79	.03	.04	.01	-.02
293	35	15.0	-.81	.04	.05	-.12	.15
294	35	30.0	-.83	.05	.06	-.24	.29
295	35	45.0	-.86	.10	.12	-.30	.35
296	35	60.0	-.60	.09	.15	-.11	.18
297	35	75.0	-.27	.02	.09	.06	-.23
298	35	90.0	-.08	-.00	-.03	.10	-1.19
299	35	105.0	.05	.02	-.39	.20	3.89
300	35	120.0	.29	.06	-.21	.31	1.08
301	35	135.0	.46	.07	-.16	.34	.72
302	35	150.0	.50	.06	-.12	.25	.51
303	35	165.0	.51	.07	-.13	.14	.28
304	35	180.0	.48	.06	-.13	.02	.04

## DATA FOR FILE : S15

PUN	CONF	WIND	CN	CMZ	ES	CMS	EZ
99	35	0.0	-.75	-.00	-.00	.03	-.04
100	35	15.0	-.76	-.00	-.00	-.06	.08
101	35	30.0	-.78	.01	.01	-.18	.23
112	35	45.0	-.81	.06	.08	-.27	.34
103	35	60.0	-.58	.09	.15	-.09	.16
104	35	75.0	-.30	.02	.06	.05	-.17
105	35	90.0	-.06	-.00	-.01	.06	-1.07
106	35	105.0	.07	.02	-.25	.18	2.71
107	35	120.0	.30	.07	-.22	.30	.99
108	35	135.0	.41	.08	-.20	.27	.65
109	35	150.0	.45	.08	-.18	.19	.43
110	35	165.0	.49	.09	-.19	.09	.19
111	35	180.0	.48	.09	-.19	.02	.03

## DATA FOR FILE : NQA1

RUN	CONF	WIND	CN	CMZ	ES	CMS	EZ
148	35	0.0	-.74	-.03	-.04	.08	-.10
149	35	30.0	-.79	-.03	-.04	-.17	.21
150	35	45.0	-.79	.01	.01	-.21	.26
151	35	60.0	-.54	.04	.08	-.08	.15

## DATA FOR FILE : NFA1

RUN	CONF	WIND	CN	CMZ	ES	CMS	EZ
147	35	0.0	-.14	-.01	-.06	.01	-.04
146	35	30.0	-.11	-.00	-.04	.01	-.07
145	35	45.0	-.14	.01	.05	-.05	.36
144	35	60.0	-.20	.01	.03	.07	-.34

## DATA FOR FILE : NQA2

RUN	CONF	WIND	CN	CMZ	ES	CMS	EZ
140	35	0.0	-.12	-.05	-.37	.00	-.03
141	35	30.0	-.38	-.04	-.09	.02	-.04
142	35	45.0	-.44	-.02	-.04	-.16	.37
143	35	60.0	-.44	.03	.06	-.15	.34

## DATA FOR FILE : NFA2

RUN	CONF	WIND	CN	CMZ	ES	CMS	EZ
138	35	0.0	-.07	-.00	-.04	-.01	.15
137	35	30.0	-.12	-.00	-.00	-.03	.27
136	35	45.0	-.27	.01	.02	.02	-.09
135	35	60.0	-.14	-.00	-.00	.02	-.13

## DATA FOR FILE : NOA3

RUN	CONF	WIND	CN	CMZ	ES	CMS	EZ
130	35	0.0	-.07	.00	.01	-.02	.31
129	35	30.0	-.28	-.03	-.11	-.06	.21
128	35	45.0	-.38	-.02	-.05	-.17	.45
127	35	60.0	-.39	.03	.07	-.13	.33

## DATA FOR FILE : NFA3

RUN	CONF	WIND	CN	CMZ	ES	CMS	EZ
131	35	0.0	-.08	-.00	-.04	-.01	.17
132	35	30.0	-.30	.00	.01	-.11	.37
133	35	45.0	-.26	-.00	-.02	.08	-.29
134	35	60.0	-.14	-.01	-.05	.03	-.23

## DATA FOR FILE : NOA7

RUN	CONF	WIND	CN	CMZ	ES	CMS	EZ
234	35	0.0	-.21	.01	.05	-.05	.23
233	35	30.0	-.34	-.01	-.04	-.10	.30
232	35	45.0	-.46	-.01	-.03	-.20	.43
231	35	60.0	-.41	.03	.08	-.14	.35

## DATA FOR FILE : NFA7

RUN	CONF	WIND	CN	CMZ	ES	CMS	EZ
235	35	0.0	-.19	-.01	-.07	-.02	.13
236	35	30.0	-.30	-.02	-.06	.05	-.18
237	35	45.0	-.14	.01	.05	-.01	.07
230	35	60.0	-.14	.00	.01	-.02	.14

## DATA FOR FILE : NOB1

RUN	CONF	WIND	CN	CMZ	ES	CMS	EZ
186	35	0.0	-.72	-.04	-.05	.06	-.08
185	35	30.0	-.62	-.00	-.00	-.10	.16
184	35	45.0	-.52	-.03	-.05	.01	-.02
183	35	60.0	-.31	-.01	-.04	.07	-.24

## DATA FOR FILE : NFB1

RUN	CONF	WIND	CN	CMZ	ES	CMS	EZ
179	35	0.0	-.15	.00	.01	-.00	.03
180	35	30.0	-.11	-.00	-.04	-.02	.19
181	35	45.0	-.09	-.01	-.10	-.03	.28
182	35	60.0	-.09	-.00	-.03	.03	-.30

## DATA FOR FILE : NOB2

RUN	CONF	WIND	CN	CMZ	ES	CMS	EZ
178	35	0.0	-.14	-.04	-.31	.00	-.01
177	35	30.0	-.27	-.01	-.03	.01	-.02
176	35	45.0	-.17	-.01	-.04	.28	-1.66
175	35	60.0	-.16	-.02	-.12	.05	-.28

## DATA FOR FILE : NFB2

RUN	CONF	WIND	CN	CMZ	ES	CMS	EZ
171	35	0.0	-.09	.01	.09	-.00	.05
172	35	30.0	-.07	-.00	-.03	.00	-.06
173	35	45.0	-.10	-.02	-.17	.09	-.89
174	35	60.0	-.24	.02	.07	.06	-.25

## DATA FOR FILE : NOB3

RUN	CONF	WIND	CN	CMZ	ES	CMS	EZ
170	35	0.0	-.03	.00	.05	-.01	.36
169	35	30.0	-.16	-.00	-.00	.11	-.69
168	35	45.0	-.14	-.01	-.10	.12	-.85
167	35	60.0	-.15	-.01	-.09	.06	-.40

## DATA FOR FILE : NFB3

RUN	CONF	WIND	CN	CMZ	ES	CMS	EZ
163	35	0.0	-.07	.00	.02	.00	-.01
164	35	30.0	-.09	-.01	-.09	.06	-.70
165	35	45.0	-.26	-.01	-.04	.05	-.18
166	35	60.0	-.28	.00	.01	.04	-.14

## DATA FOR FILE : NOB4

RUN	CONF	WIND	CN	CMZ	ES	CMS	EZ
162	35	0.0	-.05	.02	.38	-.03	.59
161	35	30.0	-.23	-.01	-.03	.03	-.12
160	35	45.0	-.16	-.00	-.03	.14	-.87
159	35	60.0	-.16	-.01	-.07	.05	-.33

## DATA FOR FILE : NFB4

RUN	CONF	WIND	CN	CMZ	ES	CMS	EZ
155	35	0.0	-.15	-.01	-.04	-.02	.11
156	35	30.0	-.18	-.01	-.04	.05	-.27
157	35	45.0	-.33	-.00	-.00	.01	-.02
158	35	60.0	-.20	-.01	-.03	.02	-.10

## DATA FOR FILE : NDC1

RUN	CONF	WIND	CN	CMZ	ES	CMS	EZ
227	35	0.0	-.71	-.04	-.05	.04	-.05
226	35	30.0	-.63	-.02	-.03	-.05	.09
225	35	45.0	-.51	-.02	-.03	.01	-.02
224	35	60.0	-.32	-.02	-.08	.15	-.46

## DATA FOR FILE : NFC1

RUN	CONF	WIND	CN	CMZ	ES	CMS	EZ
220	35	0.0	-.19	-.01	-.06	-.00	.01
221	35	30.0	-.15	-.00	-.01	-.02	.11
222	35	45.0	-.11	-.01	-.10	.01	-.06
223	35	60.0	-.08	.00	.03	.04	-.46

## DATA FOR FILE : NDC2

RUN	CONF	WIND	CN	CMZ	ES	CMS	EZ
211	35	0.0	-.09	-.04	-.43	.01	-.07
212	35	30.0	-.12	-.03	-.23	-.00	.04
213	35	45.0	-.15	-.02	-.13	-.02	.13
214	35	60.0	-.08	.00	.02	.19	-2.28

## DATA FOR FILE : NFC2

RUN	CONF	WIND	CN	CMZ	ES	CMS	EZ
219	35	0.0	-.11	-.00	-.04	.00	-.01
217	35	30.0	-.06	-.00	-.02	-.00	.00
216	35	45.0	-.07	-.01	-.09	.03	-.47
215	35	60.0	-.08	-.01	-.08	.10	-1.27



## DATA FOR FILE : NDC3

RUN	CONF	WIND	CN	CMZ	ES	CMS	EZ
210	35	0.0	-.07	-.01	-.07	-.00	.05
209	35	30.0	-.11	-.01	-.12	-.00	.01
208	35	45.0	-.11	.01	.08	.11	-1.00
207	35	60.0	-.06	.00	.01	.13	-1.96

## DATA FOR FILE : NFC3

RUN	CONF	WIND	CN	CMZ	ES	CMS	EZ
203	35	0.0	-.07	.01	.09	-.00	.05
204	35	30.0	-.09	.00	.03	.01	-.14
205	35	45.0	-.09	-.01	-.16	.09	-.96
206	35	60.0	-.16	-.00	-.00	.07	-.41

## DATA FOR FILE : NDC4

RUN	CONF	WIND	CN	CMZ	ES	CMS	EZ
195	35	0.0	-.08	.00	.01	-.01	.08
196	35	30.0	-.10	-.00	-.02	.06	-.60
197	35	45.0	-.11	.00	.01	.06	-.60
198	35	60.0	-.06	-.00	-.04	.13	-2.21

## DATA FOR FILE : NFC4

RUN	CONF	WIND	CN	CMZ	ES	CMS	EZ
202	35	0.0	-.11	.00	.03	-.00	.02
201	35	30.0	-.10	.01	.10	.03	-.35
200	35	45.0	-.12	.00	.02	.06	-.52
199	35	60.0	-.17	-.00	-.00	.05	-.31

## DATA FOR FILE : NDC7

RUN	CONF	WIND	CN	CMZ	ES	CMS	EZ
194	35	0.0	-.14	-.00	-.02	-.01	.06
347	35	30.0	-.14	.00	.00	-.03	-.22
192	35	45.0	-.13	-.00	-.02	.06	-.50
189	35	60.0	-.06	.00	.02	.14	-2.13

## DATA FOR FILE : NFC7

RUN	CONF	WIND	CN	CMZ	ES	CMS	EZ
348	35	0.0	-.14	-.00	.02	-.02	.02
349	35	30.0	-.17	-.00	.02	.04	-.25
191	35	45.0	-.20	.01	.04	.04	-.22
187	35	60.0	-.14	.00	.03	.00	-.03

## DATA FOR FILE : SOA1

RUN	CONF	WIND	CN	CMZ	ES	CMS	EZ
252	35	180.0	.48	.09	-.18	.03	.07
251	35	210.0	.53	.08	-.16	-.23	-.43
250	35	225.0	.46	.08	-.18	-.30	-.66

## DATA FOR FILE : SFA1

RUN	CONF	WIND	CN	CMZ	ES	CMS	EZ
253	35	180.0	.06	-.00	.01	.02	.31
254	35	210.0	.08	-.00	.01	-.05	-.57
255	35	225.0	.16	-.01	.06	-.10	-.62

## DATA FOR FILE : SOA2

RUN	CONF	WIND	CN	CMZ	ES	CMS	EZ
247	35	180.0	-.07	-.00	-.05	-.05	.83
248	35	210.0	.20	.01	-.06	-.35	-1.76
249	35	225.0	.30	.03	-.09	-.46	-1.52

## DATA FOR FILE : SFA2

RUN	CONF	WIND	CN	CMZ	ES	CMS	EZ
246	35	180.0	-.04	-.01	-.21	-.01	.40
245	35	210.0	.15	-.01	.07	-.17	-1.12
244	35	225.0	.27	-.00	.01	-.20	-.73

## DATA FOR FILE : SOA3

RUN	CONF	WIND	CN	CMZ	ES	CMS	EZ
240	35	180.0	.02	-.00	.15	-.08	-3.27
239	35	210.0	.25	.01	-.02	-.31	-1.23
238	35	225.0	.31	.02	-.05	-.40	-1.29

## DATA FOR FILE : SFA3

RUN	CONF	WIND	CN	CMZ	ES	CMS	EZ
241	35	180.0	-.01	-.01	-.65	-.02	9.99
242	35	210.0	.27	-.01	.05	-.25	-.93
243	35	225.0	.26	-.01	.02	-.21	-.79

## DATA FOR FILE : SOB1

RUN	CONF	WIND	CN	CMZ	ES	CMS	EZ
271	35	180.0	.52	.08	-.15	-.03	-.06
272	35	210.0	.44	.09	-.20	-.17	-.39
273	35	225.0	.35	.07	-.20	-.18	-.50

## DATA FOR FILE : SFB1

RUN	CONF	WIND	CN	CMZ	ES	CMS	EZ
270	35	180.0	.08	.01	-.08	.00	.01
269	35	210.0	.03	.00	-.05	-.00	-.08
268	35	225.0	-.08	.00	.01	-.06	.68

## DATA FOR FILE : SOB2

RUN	CONF	WIND	CN	CMZ	ES	CMS	EZ
264	35	180.0	-.02	-.01	-.62	.01	-.36
263	35	210.0	.03	.00	-.10	-.05	-1.90
262	35	225.0	.02	.02	-.94	-.07	-2.67

## DATA FOR FILE : SFB2

RUN	CONF	WIND	CN	CMZ	ES	CMS	EZ
265	35	180.0	-.01	-.00	-.36	.01	9.99
266	35	210.0	-.04	.00	.00	-.05	1.30
267	35	225.0	.02	-.01	.01	-.13	9.99

## DATA FOR FILE : SOB3

RUN	CONF	WIND	CN	CMZ	ES	CMS	EZ
259	35	180.0	-.01	-.02	-2.00	.02	9.99
260	35	210.0	.08	.00	-.02	-.06	-.78
261	35	225.0	.01	.01	-.98	.06	9.99

## DATA FOR FILE : SFB3

RUN	CONF	WIND	CN	CMZ	ES	CMS	EZ
258	35	180.0	-.01	-.01	-.95	.01	9.99
257	35	210.0	.01	-.02	1.39	-.12	9.99
256	35	225.0	.07	-.02	.28	-.09	-1.25

## DATA FOR FILE : SOC1

RUN	CONF	WIND	CN	CMZ	ES	CMS	EZ
288	35	180.0	.51	.08	-.15	-.05	-.10
287	35	210.0	.46	.09	-.19	-.21	-.45
286	35	225.0	.35	.07	-.20	-.13	-.38

## DATA FOR FILE : SFC1

RUN	CONF	WIND	CN	CMZ	ES	CMS	EZ
289	35	180.0	.08	.00	-.01	.01	.10
290	35	210.0	.04	.01	-.22	-.02	-.60
291	35	225.0	-.02	-.00	-.12	-.02	.73

## DATA FOR FILE : SOC2

RUN	CONF	WIND	CN	CMZ	ES	CMS	EZ
283	35	180.0	-.07	-.02	-.25	.01	-.14
284	35	210.0	-.05	-.00	-.02	-.02	.30
285	35	225.0	-.03	.00	.08	-.04	1.52

## DATA FOR FILE : SFC2

RUN	CONF	WIND	CN	CMZ	ES	CMS	EZ
262	35	180.0	-.02	-.00	-.08	.01	-.34
261	35	210.0	-.02	-.00	-.04	-.02	.77
260	35	225.0	-.10	.01	.08	-.04	.36

## DATA FOR FILE : SOC3

RUN	CONF	WIND	CN	CMZ	ES	CMS	EZ
276	35	180.0	.00	-.00	1.65	-.00	9.99
275	35	210.0	-.02	-.00	-.06	-.06	2.80
274	35	225.0	.01	.00	-.15	-.06	9.99

## DATA FOR FILE : SFC3

RUN	CONF	WIND	CN	CMZ	ES	CMS	EZ
277	35	180.0	-.01	-.01	-1.48	.01	9.99
278	35	210.0	-.03	-.01	-.17	-.03	.86
279	35	225.0	-.04	-.01	-.22	-.05	1.19